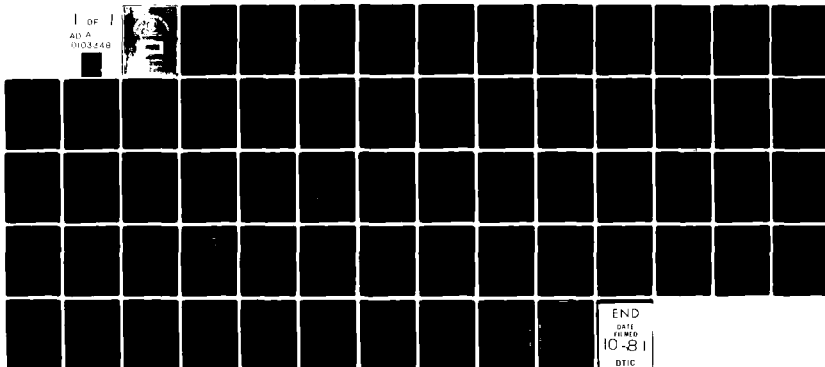


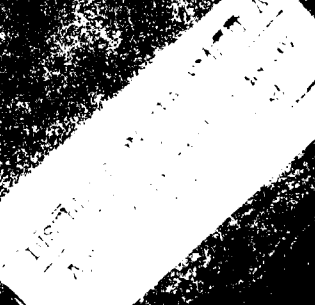
AD-A103 348 AIR FORCE INST OF TECH WRIGHT-PATTERSON AFB OH SCH00--ETC F/G 20/5  
ANALYSIS OF XEC1 EMISSION IN A HOLLOW CATHODE DISCHARGE.(U)  
JUN 81 G A VOGEL  
UNCLASSIFIED AFIT/GEP/PH/81-6 NL

1 OF 1  
AD-A  
0103348



END  
DATE  
FILMED  
10-81  
DTIC

FL



(1)

DTIC  
TE  
AUG 26 1981  
H

ANALYSIS OF  $\text{XeCl}$  EMISSION  
IN A HOLLOW CATHODE DISCHARGE,  
THESIS

AFIT/GEP/PH ✓ George A. Vogel  
81-6

ANALYSIS OF XeCl EMISSION IN  
A HOLLOW CATHODE DISCHARGE  
THESIS

Presented to the Faculty of the School of Engineering  
of the Air Force Institute of Technology  
Air University  
in Partial Fulfillment of the  
Requirements for the Degree of  
Master of Science

by

George A. Vogel  
Graduate Engineering Physics

June 1981

### Acknowledgements

I would like to express my thanks to the many fine people who helped in this thesis project. I would like to thank my advisor Dr. Alan Garscadden for his time, patience, and enlightening instruction. A special note of thanks goes to Mr. Charles DeJoseph who saved me many hours of frustration by sharing his knowledge and experience in the areas of spectroscopy and high vacuum technology. I would also like to thank my supervisor, Larry J. Baumgardner, for allowing me to perform much of this work as part of my job, Mrs. Judy Tislow for typing this thesis, and last but not least my wife and children who put up with many unfinished projects while I worked on this thesis.

George A. Vogel

|                    |         |  |
|--------------------|---------|--|
| Accession For      |         | <input checked="checked" type="checkbox"/> |
| NTIS               | CSA&I   | <input type="checkbox"/>                   |
| DTIC               | TIR     | <input type="checkbox"/>                   |
| Unannounced        |         | <input type="checkbox"/>                   |
| Justification      |         |  |
| By                 |         |  |
| Distribution/      |         |  |
| Availability Codes |         |  |
| Avail and/or       |         |  |
| Dist               | Special |  |
| A                  |         |  |

## Table of Contents

|  | Page |
|--|------|
| Acknowledgements . . . . .                       | ii   |
| List of Figures . . . . .                        | iv   |
| List of Tables . . . . .                         | v    |
| Abstract . . . . .                               | vi   |
| I. Introduction . . . . .                        | 1    |
| Glow Discharge . . . . .                         | 2    |
| Hollow Cathode . . . . .                         | 5    |
| Excimers . . . . .                               | 8    |
| XeCl* in the Hollow Cathode . . . . .            | 10   |
| II. Experimental Program . . . . .               | 12   |
| Scope . . . . .                                  | 12   |
| Experimental Apparatus . . . . .                 | 12   |
| Experimental Techniques . . . . .                | 21   |
| III. Theory . . . . .                            | 23   |
| Hollow Cathode Discharge Model . . . . .         | 23   |
| Primary Reactions . . . . .                      | 26   |
| Rate Equations . . . . .                         | 28   |
| IV. Analysis and Discussion of Results . . . . . | 34   |
| XeCl* Spectral Characteristics . . . . .         | 34   |
| Dominant Reactions . . . . .                     | 34   |
| Results . . . . .                                | 40   |
| V. Summary and Conclusions . . . . .             | 48   |
| VI. Recommendations . . . . .                    | 50   |
| Bibliography . . . . .                           | 52   |
| Vita . . . . .                                   | 54   |

# List of Figures

| <u>Figure</u> |   | <u>Page</u> |
|---------------|---|-------------|
| 1             | Glow Discharge . . . . .  | 3           |
| 2             | Hollow Cathode Discharge . . . . .  | 7           |
| 3             | Potential Energy Diagram for AB* Excimer . . . . .  | 9           |
| 4             | Hollow Cathode Construction . . . . .   | 13          |
| 5             | Vacuum System and Gas Supply . . . . .  | 15          |
| 6             | High Voltage Electrical System . . . . .  | 17          |
| 7             | Optical and Electrical Layout . . . . .   | 19          |
| 8             | Hollow Cathode Discharge Model . . . . .  | 24          |
| 9             | Dominant Mechanisms for Production of XeCl* in a Hollow<br>Cathode Two-Component Rare-Gas-Halide System at Pressures<br>of 1-4 Torr . . . . . | 29          |
| 10            | Calculated Potential Curves for XeCl . . . . .  | 35          |
| 11            | XeCl* Spectrum 200-500 nm . . . . .   | 36          |
| 12            | Relative XeCl* Output vs Total Discharge Current . . . . .  | 41          |
| 13            | Relative XeCl* Output vs Discharge Voltage in Hollow<br>Cathode with Ne/Xe = 1/1 . . . . .  | 43          |
| 14            | Relative XeCl* Output vs Discharge Voltage in Hollow<br>Cathode with Ne/Xe = 5/1 . . . . .  | 44          |
| 15            | Relative XeCl* Output vs Percent Xenon in Hollow Cathode . . . .  | 47          |

List of Tables

| <u>Table</u> |  | <u>Page</u> |
|--------------|--|-------------|
| I            | Possible Rare Gas-Halogen Excimers, with Wavelengths of Known Laser Transitions Given in Nanometers . . . . .  | 10          |
| II           | Experimental Gases . . . . .   | 16          |
| III          | Summary of Primary Reactions in Hollow Cathode Discharge Containing Ne, Xe, HCl . . . . .  | 30          |
| IV           | Calculated and Experimental Emission Energies ( $\Delta E$ ), Wavelengths ( $\lambda$ ), and Lifetimes ( $\tau$ ) for Ionic-Covalent Transitions in XeCl . . . . . | 35          |



### Abstract

This work investigates the characteristics of a hollow cathode discharge containing neon, xenon, and hydrogen chloride gases. The line intensity of the XeCl excimer spontaneous emission (308 nm) is measured as a function of excitation current and the partial pressures of Xe and HCl.

The hollow cathode, operating with constant discharge current, produces relatively intense XeCl emission and provides a stable discharge, in spite of the presence of the electronegative Cl ions. Measurements were made for total pressures of 4, 2, and 1 torr, 0, 2, 4, and 8 percent HCl, and mixes of Ne/Xe from 100% Ne to 100% Xe.

The hollow cathode provides a unique discharge characteristic by providing both 200 - 400 ev "beam like" electrons and high densities ( $10^{12}/\text{cm}^3$ ) of low energy ( $700^\circ\text{K}$ ) electrons. A simple model is developed for the hollow cathode discharge by assuming the electrons are only in these two energy groups. This model is coupled with the dominant chemical processes and is used to explain the behavior of the discharge with direct current excitation.

The results of both analysis and measurements show the XeCl emission to be proportional to Xe concentration, HCl concentration, and discharge current. These results indicate that the primary formation process of the XeCl excimer in the hollow cathode is due to the combination of Xe and Cl ions.

## I. Introduction

In the development of new gaseous laser systems, it is often necessary to thoroughly study the potential mixes of candidate materials with varied electrical discharge techniques and conditions. While each different discharge technique evokes its own unique set of complex discharge characteristics, these different characteristics help emphasize different aspects of the materials' nature. As the electrical discharge behavior of a potential gas laser mix becomes better known, the easier it becomes to optimize the laser output by modifying its discharge conditions.

The AF Wright Aeronautical Laboratories, Energy Conversion Branch at Wright-Patterson AFB, OH, where work on this thesis was performed, is currently engaged in experimental work on the development of various laser systems. One particular laser being developed there is a xenon-chloride excimer ( $\text{XeCl}^*$ ) laser operating in a closed cycle pulsed electrical discharge system. This thesis investigates the characteristics of a possible gas mixture for this laser using a hollow cathode discharge. For a better understanding of this problem, the concepts of the glow discharge, hollow cathode discharge, and excimers are briefly presented before a more detailed statement of the problem is given.

Glow Discharge (Ref 1: 217-221)

When a direct-current glow discharge is established in a long cylindrical tube which is filled with a rare gas at a pressure of between 0.1 and 1 torr, the visible light emitted from the discharge is distributed over the length of the tube as shown in figure 1. Starting at the cathode there exists sometimes a very narrow dark space (Aston's) close to it followed by a thin relatively feeble sheath luminous layer -- the cathode glow -- which in turn is followed by the cathode dark space. Aston's dark space and the cathode glow are not always clearly visible. A sharp boundary separates the cathode dark space from the negative glow, which becomes progressively dimmer towards the Faraday dark space. At the positive end of this region is the positive column. It is either a region of uniform luminosity or regularly striated. At the positive end of the positive column there is sometimes visible an anode dark space followed by the anode glow close to the anode itself.

The transport of current through a glow discharge occurs by the axial motion of electrons and positive ions. The flow of current through the cathode zones can be understood by referring to the distribution of the electric field, that is its axial component, as shown in figure 1. The field has been found to be large at the cathode, decreasing in intensity towards the negative glow, and, after passing a minimum in the Faraday dark space, it stays constant throughout the positive column and only rises again at the anode.

Consider an electron emitted from the cathode, for example by a positive ion which impinges on it. This electron is first accelerated in a strong field, but initially it executes few ionizing collisions because

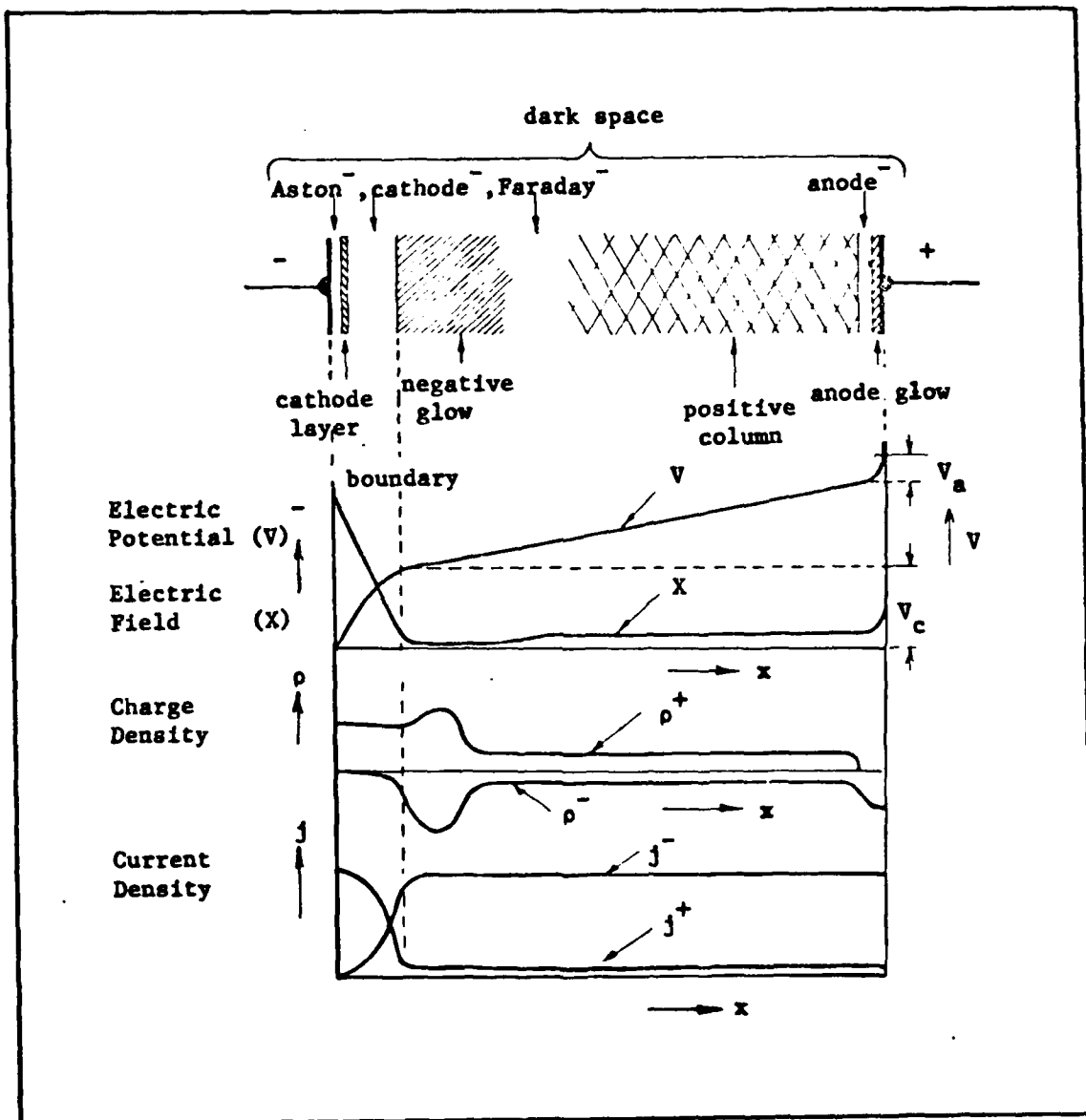


Figure 1. Glow Discharge (Ref 1: 218)

its energy is not sufficiently far above ionization potential. However, further from the cathode, though the field has become weaker, the electron ionizes more efficiently and strong electron multiplication will take place. Near the boundary between the cathode dark space and the negative glow the field has become very weak, and thus only the fast electrons which have not lost energy by inelastic collisions will be able to ionize in that region. However, a large number of electrons will cross the boundary and enter the negative glow.

Due to ionization the number of electrons able to ionize has increased between the cathode and the glow boundary, and a large number of positive ions has been formed representing a strong positive space charge. These positive ions will move through the cathode dark space and impinge on the cathode. Also metastable atoms, fast unexcited atoms, and radiation will fall on the cathode with the result that secondary electrons are emitted from it. In order to have a steady state, each electron which is emitted by the cathode must provide sufficient ionizations and excitations to cause the release of one further electron from the cathode.

In the uniform positive column the axial component of the electric field is also found to be uniform. It follows that the net space charge is zero or that the concentration of electrons at any point is equal to that of positive ions. Because of the small mobility of positive ions the electrons carry practically the whole discharge current while the positive ions compensate the electron space charge. The field in the positive column is several orders of magnitude smaller than that found in the dark space. This fact as well as the uniform appearance of the positive column indicates that ionization is

not obtained from the drift velocity of electrons in the field direction but rather from their large random velocity acquired by numerous elastic collisions in the electric field. The random velocity under these conditions in several orders of magnitude higher than the drift velocity.

#### Hollow Cathode

One form of glow discharge is the hollow cathode discharge. The geometry for this discharge, in its simplest form, is two plane cathodes separated by some distance  $d$ . The anode position has been found to be relatively unimportant. For large  $d$ , the discharge appears as if there are two positive columns between them, with each cathode having its own separate negative glow. As  $d$  is decreased, the positive columns disappear and the negative glows begin to merge. The current densities increase for constant discharge voltage. For small pressures and distances, for example, current densities can be  $10^2$  to  $10^3$  times larger than those of a normal positive column discharge (Ref 1: 236). This increase in current density for constant voltage, which could be called discharge efficiency, is due to a number of effects. Two major effects are enhanced secondary emission by noncharged particles and the Pendel effect (Ref 2: 460-461).

In a positive column discharge, a considerable fraction of the noncharged particles (i.e., photons and metastable excited atoms) which can produce secondary electron emission if they strike the cathode, are lost as agents for maintaining the discharge, since their motion is not affected by the electric field, and they can travel towards the tube walls or the anode. With the hollow cathode configuration, as  $d$  is reduced, an increasing proportion of these particles otherwise "lost"

to the walls will strike the cathodes instead and the total secondary emission efficiency of the discharge will rise.

The second process which also contributes to the rise in discharge efficiency, as  $d$  is reduced, is the Pendel effect. This effect is related to the oscillation of electrons from side to side of the cathode cavity, resulting from the cathode geometry and electric field configuration. This effect is likely to be particularly significant at low pressures, since an appreciable number of fast electrons may pass through the negative glow without ionizing atoms, enter the opposite cathode dark space, where the fields are high, and are repelled back into the negative glow. Ionization is enhanced since the electrons are forced to deposit their energy into a smaller volume.

The hollow cathode used for this thesis experiment has a cylindrical cathode instead of two plane cathodes. The discharge is operated in a medium-pressure region (pressures between 1 and 4 torr) where most of the electron energy is dissipated in the negative glow region and the mean free path of the primary discharge electrons is on the order of the diameter of the negative glow.

Figure 2 shows a cross-section of a typical hollow cathode discharge. The anodes, not shown in this drawing, are equally spaced at points in a longitudinal line along the surface of the cathode (see figure 4).

The negative glow is essentially a beam produced plasma generated by high energy electrons from the cathode region and, for the medium pressure case, is nearly uniform across its diameter. Measurements have shown that, with the exception of regions near the cathode, the radial and longitudinal fields are not very strong (Ref 3: 882). The cathode fall region, on the other hand, has nearly all of the discharge

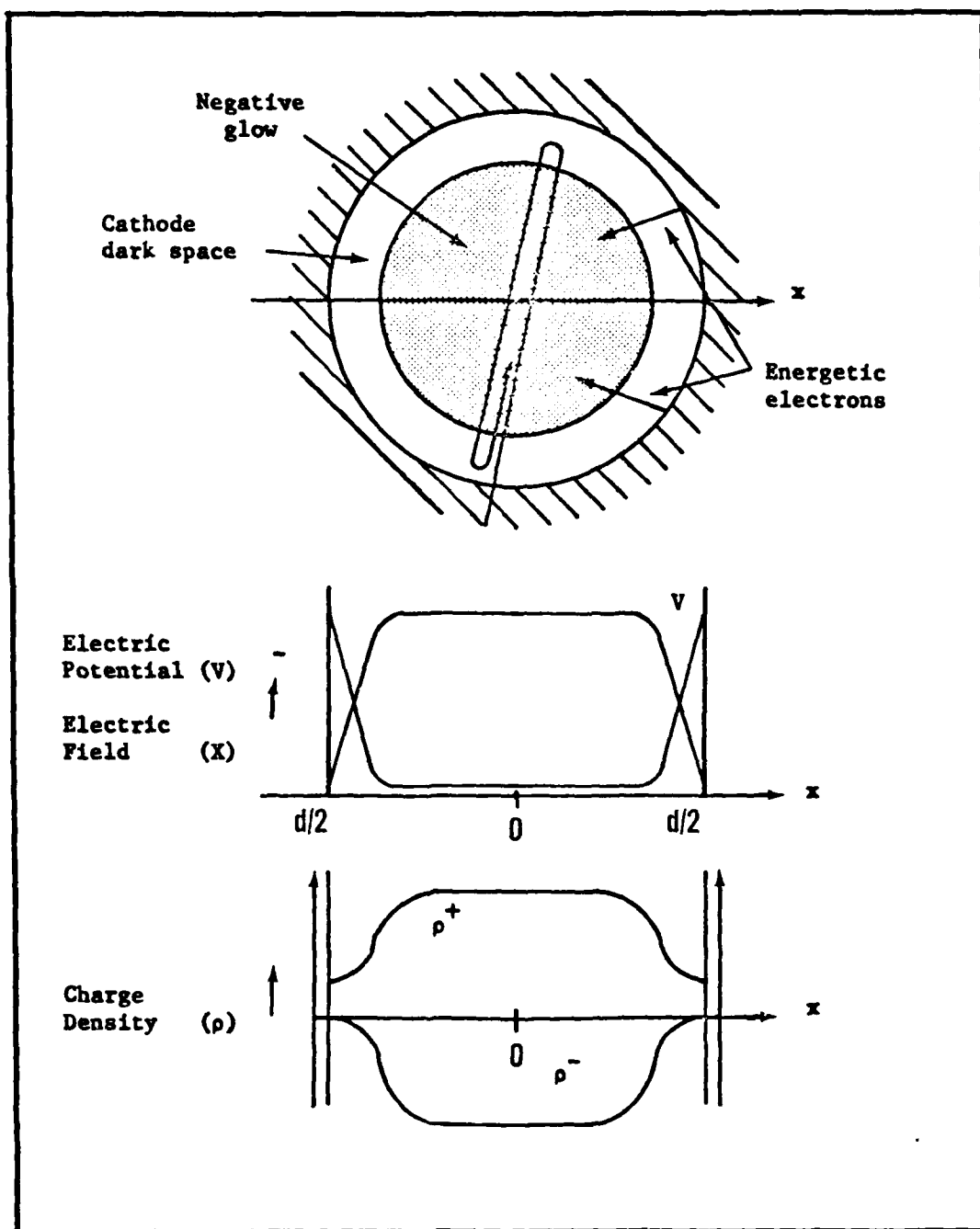


Figure 2. Hollow Cathode Discharge



voltage across itself. This is the potential which creates the beam electrons.

Excimers (Ref 4: 95-97)

The term excimer was first introduced in 1960 by Stevens & Hutton to describe a dimer which is associated or bound in an excited electronic state and which is dissociated or dissociative in the ground state. The term properly denotes an excited homopolar molecule, e.g.,  $\text{Xe}_2^*$ ,  $\text{Hg}_2^*$ . The term exciplex refers to an electronically excited heteropolar complex, e.g.,  $\text{KrF}^*$ ,  $\text{XeOH}^*$ ,  $\text{XeCl}^*$ , which is dissociative in the electronic ground state. Since the exploitation of these systems as laser media, the distinction between the two terms is frequently overlooked and both homopolar and heteropolar systems are commonly referred to as excimers,

Excimers are formed by the interaction between two atoms or molecules, one of which is excited,



Or they may be formed by two ions,



The bound molecule  $AB^*$  may then decay radiatively to the ground state,



The ground state may be repulsive or weakly bound so as to be unstable at normal temperatures,



A simple potential energy diagram for this excimer  $AB^*$  is shown in figure 3.

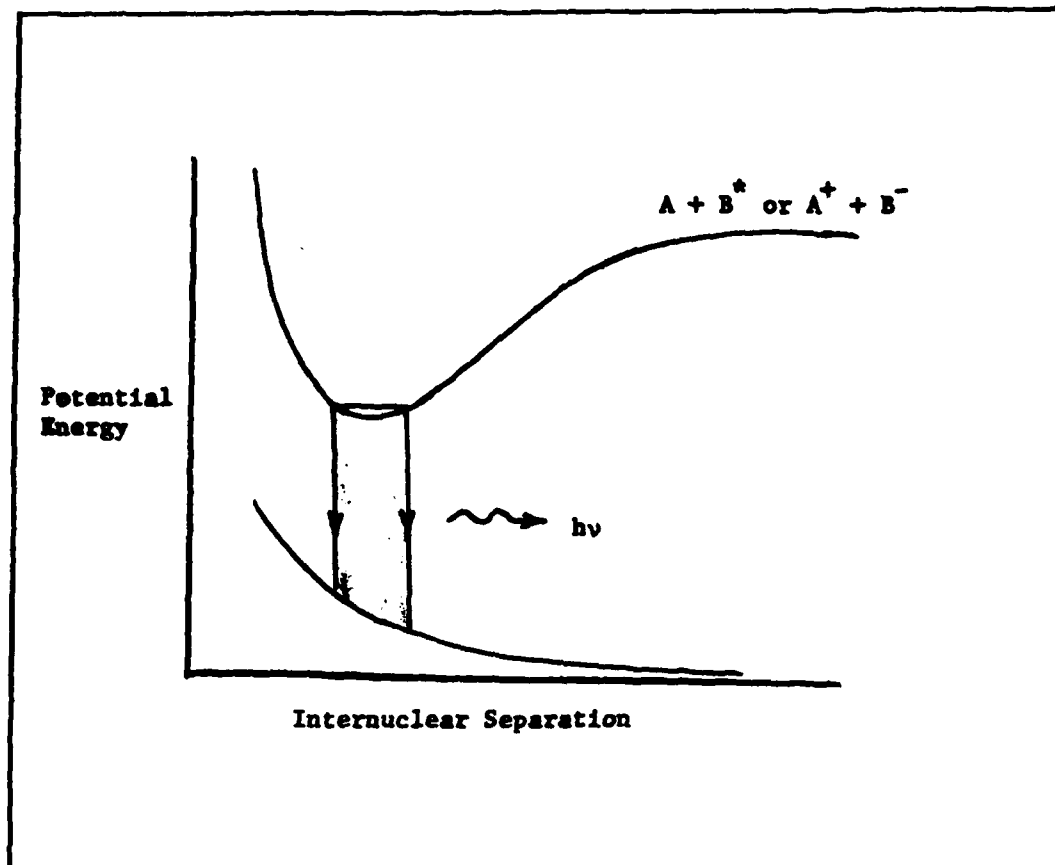


Figure 3. Potential energy diagram for  $AB^*$  excimer.

The rare gas halide excimer emissions were first broadly characterized in studies of the quenching of metastable atomic states in rare gases by halogen bearing compounds (Ref 5). Further studies showed the production of these excimer excited states to be highly efficient under the higher pressure and deposition rate conditions required for excimer laser action.

Table I shows a matrix of the possible rare gas halogen excimers, with wavelengths of known laser transitions. Lasing occurs most readily with the heavy rare gas-light halogen excimer  $XeF^*$  and becomes more

Table I

Possible rare gas-halogen excimers, with wavelengths of known laser transitions given in nanometers.

|    | He | Ne | Ar  | Kr  | Xe  |
|----|----|----|-----|-----|-----|
| F  |    |    | 193 | 248 | 351 |
| Cl |    |    | 175 | 223 | 308 |
| Br |    |    |     |     | 282 |
| I  |    |    |     |     |     |

difficult toward lighter rare gases and/or heavier halogens.

These excimers are potentially useful for lasers since the lower level dissociation time, about  $10^{-12}$  sec, is much shorter than upper level radiative lifetimes,  $10^{-9}$  to  $10^{-6}$  sec. Population inversions can be readily produced and maintained (Ref 6). In general, the excimers have the potential of efficiently generating high power pulses of radiation at ultra-violet and vacuum ultraviolet wavelengths.

#### XeCl\* in the Hollow Cathode

This work investigates the emission characteristics of a mixture of neon, xenon, and hydrogen chloride gases in a hollow cathode discharge. The objective is to parameterize the primary XeCl\* emission (308 nm) as a function of discharge current, Ne/Xe/HCl mix ratio, and total discharge pressure. By varying the mix ratio or the pressure, it is possible to identify the dominant processes which lead to the excimer formation.

The total discharge current is varied to determine how  $\text{XeCl}^*$  emission is affected by excitation rate. The hollow cathode discharge tube is selected for its simplicity of operation, ability to operate at low pressures, and ability to sustain a stable discharge in the presence of electronegative ions.

The following sections are presented as follows. Section II, Experimental Program, describes the experimental apparatus and techniques followed in the course of this work. Section III, Theory, develops a simple hollow cathode discharge model, presents the primary chemical reactions expected to be found in the discharge, and then develops the rate equations for the dominant species expected to be found in the discharge. Section IV, Analysis and Discussion of Results, describes the  $\text{XeCl}^*$  spectral characteristics and then compares the developed theory with the experimental measurements. Section V presents the summary and conclusions and Section VI gives some recommendations for future work.

## II. Experimental Program

### Scope

This section describes the experimental apparatus and techniques used during the experimental portion of this effort. The apparatus discussion divides the system into four functional groups which include the discharge tube, vacuum system/gas supply, high voltage electrical system, and the optical detecting system. The experimental techniques discussion outlines the vacuum system evacuation and filling procedures and the XeCl\* intensity measurement procedures.

### Experimental Apparatus

Discharge Tube. The hollow discharge tube shown in figure 4 is constructed from 3/8 inch O.D. 304 stainless steel tube with .070 inch wall thickness. The tube length is 24.25 inches and has 10 anodes equally spaced at 2.25 inch intervals. The anodes are constructed from 304 stainless steel with their ends recessed from the inside diameter of the discharge tube by 0.240 inches. A 0.035 inch thick alumina sleeve around the anode extends to the inside diameter of the discharge tube to prevent the anode from shorting to the cathode. The external anode feed through is insulated and sealed using a ceramic seal and adhesive.

Each anode is cooled by an aluminum block which is cooled in turn by four copper 1/4 inch tubes containing flowing tap water. The aluminum block is constructed from four pieces of aluminum, forming a sandwich and ensuring maximum surface contact with the hollow cathode, anode, and copper tube.

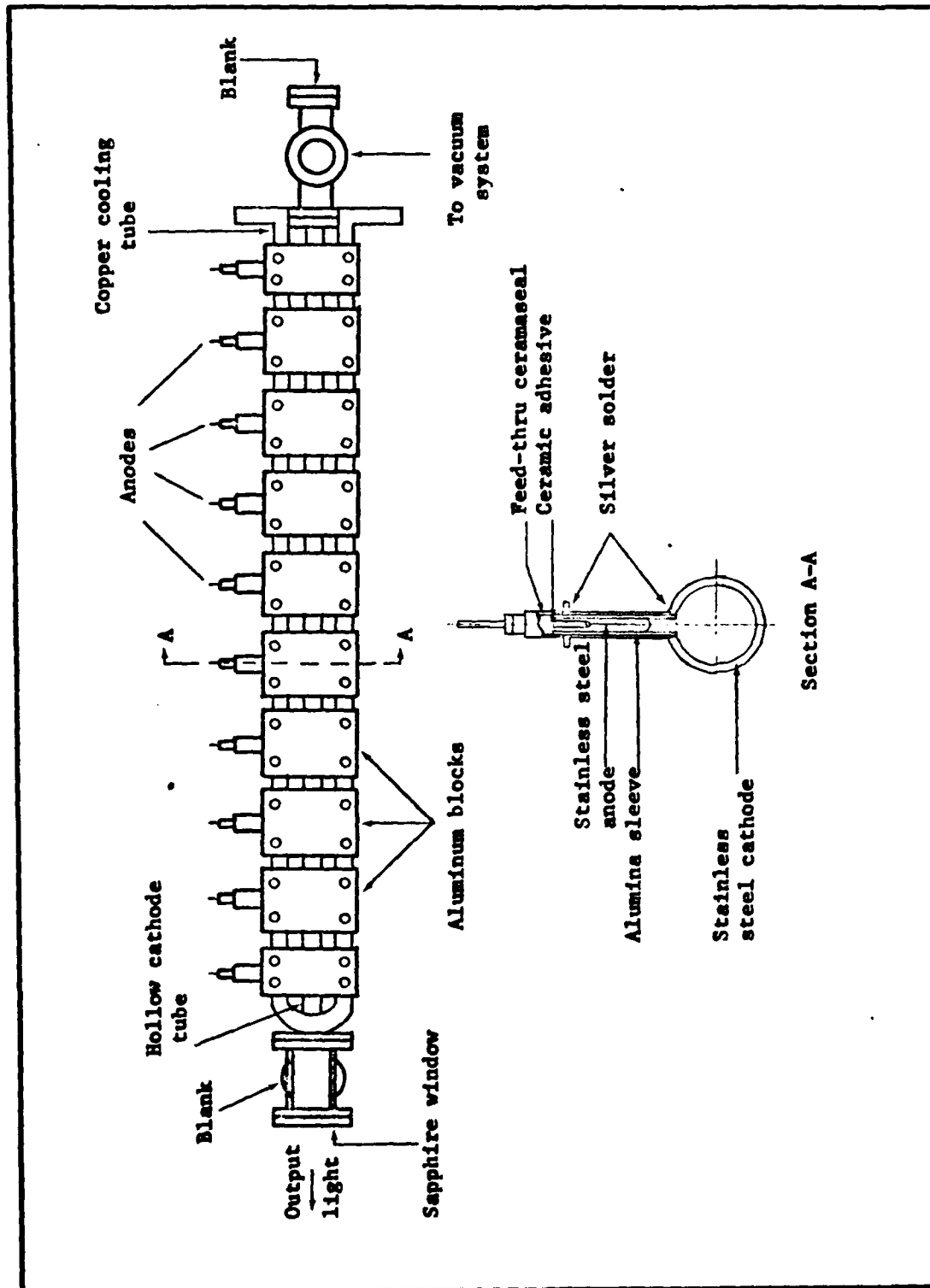


Figure 4. Hollow cathode construction.

Welded to each end of the hollow cathode tube is a mini-conflat flange. Bolted to each flange is a mini-conflat "T". On the output end of the discharge tube the "T" is terminated with a sapphire window. The port perpendicular to this is covered with a blank. The opposite end of the tube is also covered with a blank. The remaining perpendicular port is connected to the vacuum system and gas bottles with a section of flexible stainless steel vacuum line. All mini-conflat connections were sealed with copper gaskets.

Vacuum System/Gas Supply. The gas handling system is shown in figure 5. This system is constructed from stainless steel vacuum lines and fittings and used copper gaskets at all couplings. During evacuation the butterfly valve to the hollow cathode is open. The pressure within the system is dropped to 10-30 Torr by opening the copper seal bellows valve to the roughing pump. To further evacuate the system, this bellows valve is closed and the 2 inch gold seal valve is opened. The Granville-Phillips Series 205 diffusion pump with liquid nitrogen cold trap then pumps the system to a high vacuum. Vacuums of  $10^{-6}$  Torr are typically achieved.

The absolute pressure within the vacuum system is measured with one of three gauges, depending upon the system pressure. The 1000 Torr head (315 BHS-1000) to the MKS Baratron gauge is only used when the system is brought to atmospheric pressure. This gauge is not used during the experiments. The 10 Torr head (145 BHS-10) to the MKS Baratron is used throughout the experiments for measuring pressures for mixing gases and tracking total system pressure. Typical pressures measured with this head range from 0.1 to 6 Torr. When pumping with the diffusion pump, the pressure is measured with a Varian "nude" Baird-

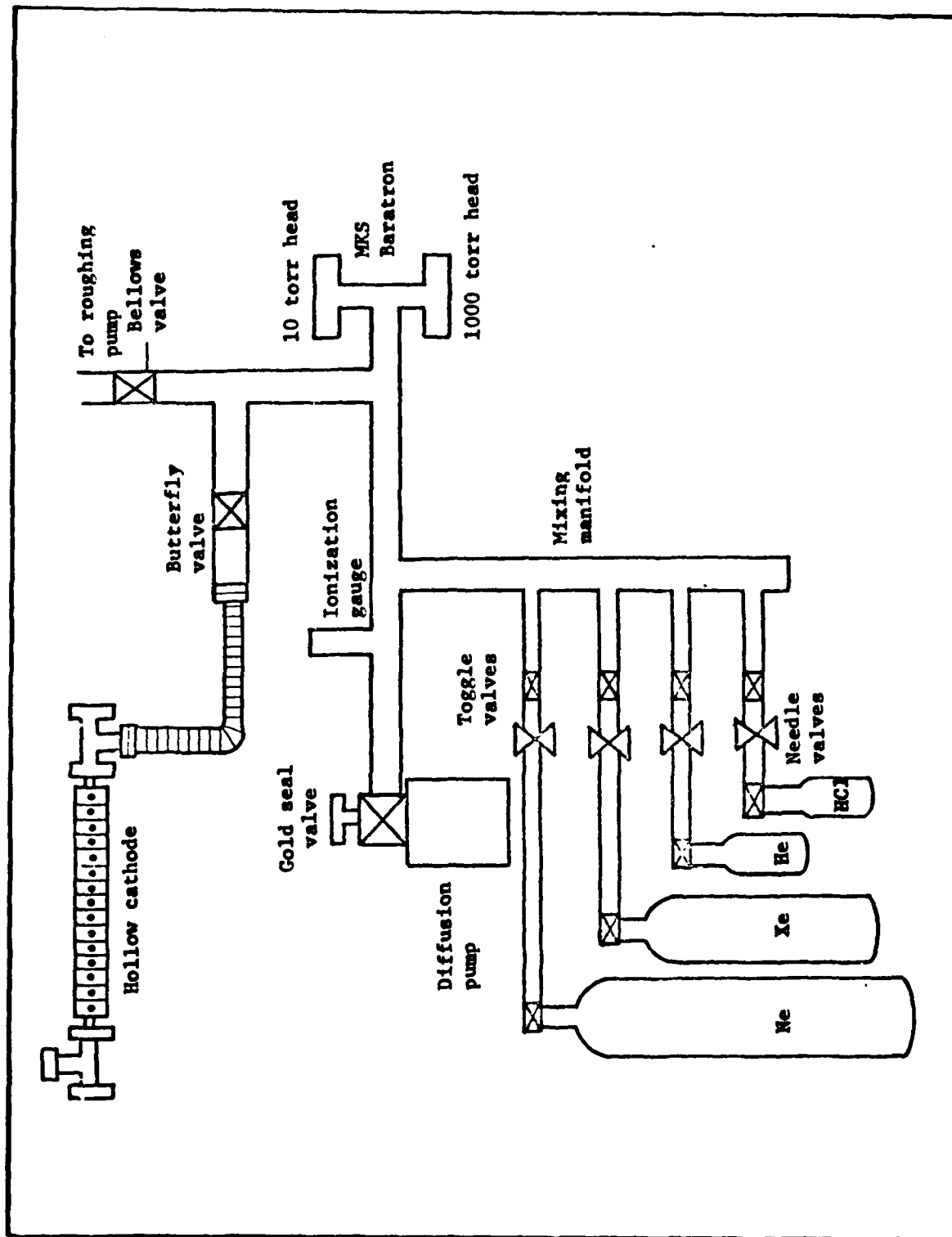


Figure 5. Vacuum system and gas supply.



Alpert ionization gauge. The gauge is read out using a Perkin-Elmer Digital Ionization gauge, Model 605-0000. The ionization gauge is used primarily for checking for leaks and verifying that the system is pumped out as well as possible.

Up to four different gas bottles can be connected to the gas manifold. Each gas line has a toggle shut-off valve and a metering needle valve. The gases used for this investigation are shown in Table II .

Table II  
Experimental Gases

| Gas | Purity                 | Manufacturer |
|-----|------------------------|--------------|
| HCl | 99% Technical Grade    | Matheson     |
| Xe  | 99.995% Research Grade | Matheson     |
| Ne  | 99.996% Grade 46       | Airco        |
| He  | 99.9999% Grade 6       | Airco        |

High Voltage Electrical System. The high voltage electrical system is shown in figure 6. High voltage is supplied by a Gregory-King Electronics 3 kv 1A DC unregulated power supply. This supply

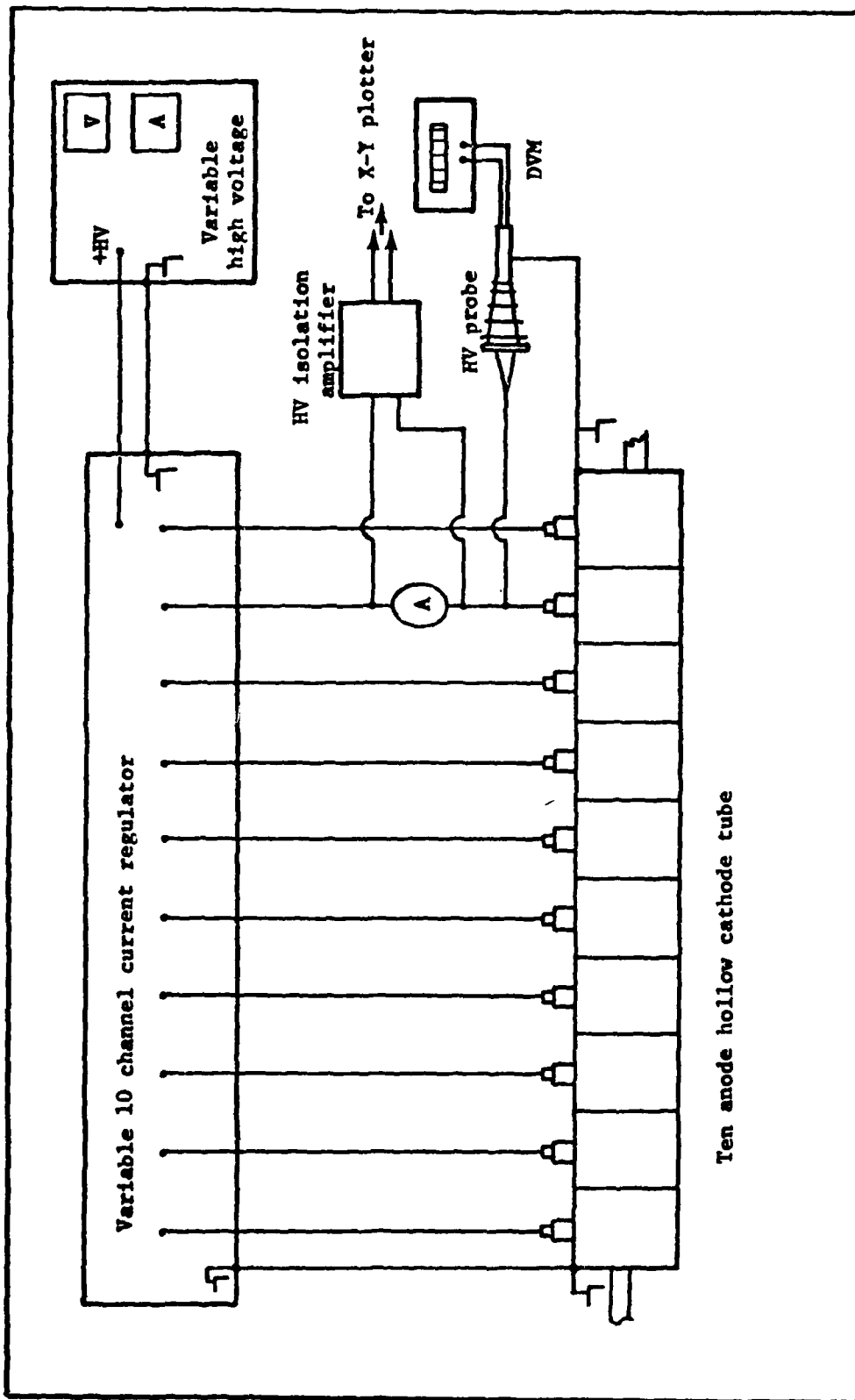


Figure 6. High voltage electrical system.

provided power for the current regulator and was typically operated at 200 to 500 volts and 0.100 and 0.500 amps total current.

The current regulator was built in-house and is capable of supplying current to ten separate circuits. The current regulation for each channel is controlled by a 10 turn potentiometer. Each potentiometer is interconnected by a plastic belt. In order to guarantee the maximum agreement in current settings between channels, each potentiometer on the belt was slipped until that channel delivered 20 milliamps. The output from each channel is connected to each anode on the hollow cathode.

The current through one of the channels is run through an ammeter to provide a measurement of discharge current. The discharge voltage is measured using the high voltage probe and digital voltmeter combination. During some of the experiments it is necessary to plot hollow cathode output intensity versus excitation current. A high voltage isolation amplifier with a gain of 100 is used for this purpose. The series resistance of the ammeter provided enough voltage drop to be amplified by the amplifier and drive the X-axis on the recorder. The X position on the plotter is thus proportional to channel current since the voltage across the ammeter is proportional to the current (assuming constant ammeter resistance).

Optical Detecting System. The optical detection system is shown in figure 7. The light emitted from the discharge along the axis of the hollow cathode is observed through the sapphire window. This radiation is imaged on the 50 $\mu$ m slit for the model 82-410 1/4 meter Jarrel Ash Monocrometer. The imaging is performed with a 10 cm focal length

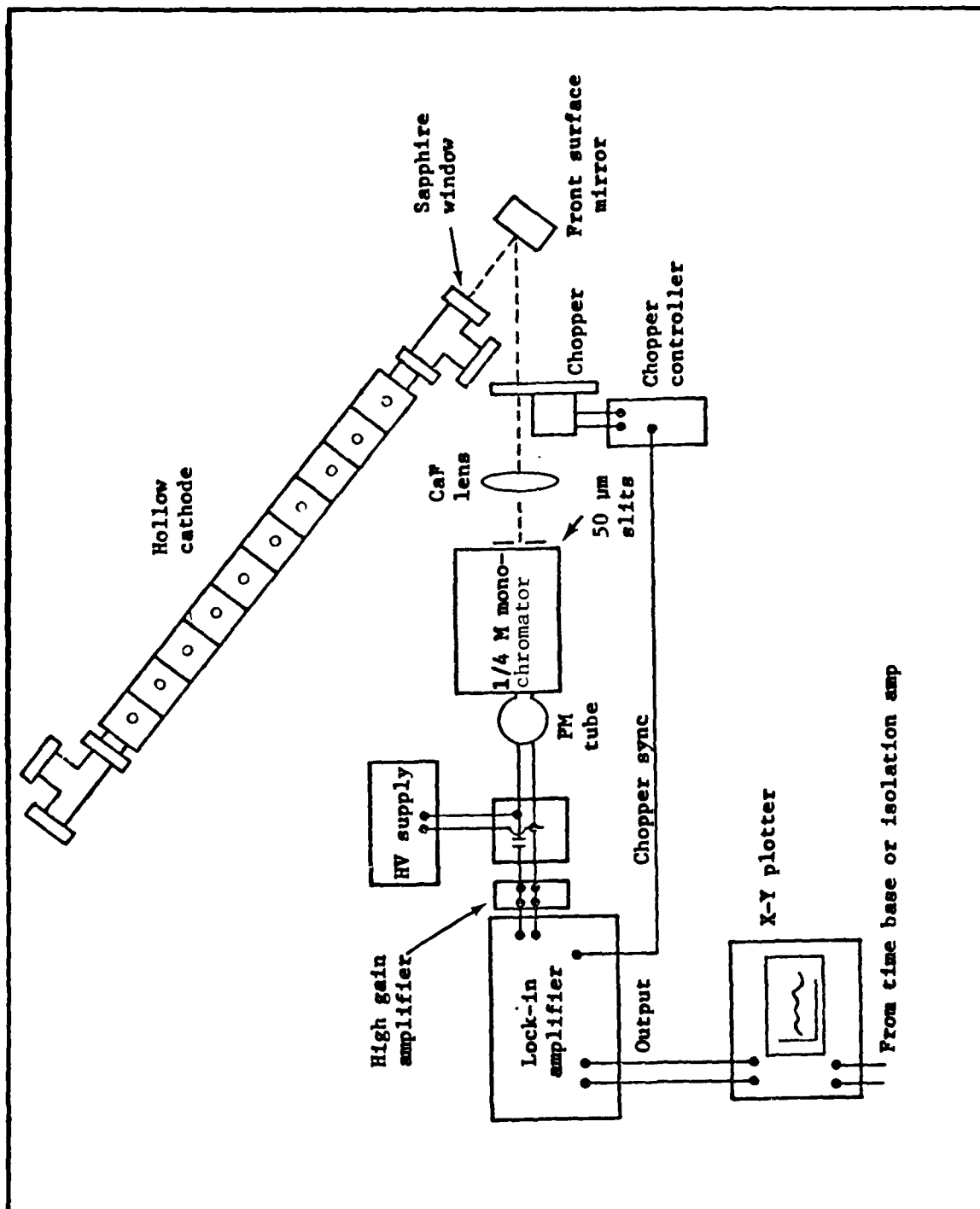


Figure 7. Optical and electrical layout.

CaF lens. To aid in the detection of the XeCl emission, a Princeton Applied Research chopper model 222 modulated the input to the monochromator.

The monochromator is used in both a scanning mode and a non-scanning mode. Scanning is performed using a 1 rpm motor and produces plots of intensity versus wavelength. The non-scanning mode is used to observe the XeCl\* 308 nm line emission intensity as a function of discharge current.

The monochromator output is detected with an LP 28 photomultiplier tube. A 50  $\mu$ m slit is also used at the input of this tube. The high voltage for the photomultiplier is supplied by a Hewlett Packard 6110A D C Power Supply. The power supply is usually set at 800 volts. The dark current of the LP 28 tube at this voltage is specified to be about 0.2 amps.

The output of the photomultiplier tube is amplified by a laboratory constructed wide band preamplifier having gains of  $10^2$  to  $10^8$ . The Princeton Applied Research Model HR-8 lock-in amplifier amplifies the inphase signal and produces a filtered output to the Y-axis of the X-Y plotter.

With the Y-axis pen position proportional to relative intensity, the X-axis of the Hewlett Packard Model 7004B X-Y plotter is used to plot either wavelength or discharge current. Wavelength is plotted when the monochromator is being scanned. The X-axis pen position is moved using the 17172A time base plug-in and is calibrated using known atomic emissions as calibration points. When 308 nm line intensity is plotted versus discharge current, the X-axis pen position is driven by the output of the high voltage isolation amplifier (see Figure 8). The Hewlett Packard 17171 ADC preamplifier is used for this condition.

### Experimental Techniques

Evacuation and Filling. Before each experiment the discharge tube and connecting vacuum lines between the toggle valves and bellows valve are pumped out to about  $10^{-5}$  Torr by the diffusion pump. These components are shown in figure 7. After a minimum of ten minutes of pumping, the gold seal valve to the diffusion pump is closed and the butterfly valve to the hollow cathode is closed.

The gases are mixed to the proper ratio in the vacuum manifold using the needle valves and the MKS Baratron gauge. Usually the HCl is allowed in first and then the Xe is added to give the proper Xe/HCl ratio. The total pressure for this initial mix is about 4 Torr. These two gases are allowed to mix for a minimum of a minute before they are pumped down through the bellows valve to the proper total pressure. The buffer gas, Ne, is then added to bring the total pressure back up to 6 Torr. This new mixture, now at the proper mix ratio, is again allowed to sit for over a minute before the bellows valve to the hollow cathode is opened. The total system pressure is brought down to 4 Torr using the bellows valve as before. The butterfly valve is then closed and the experiment ready to proceed.

Intensity Measurements. The output of the experiment is the measurement of the  $\text{XeCl}^*$  emissions as a function of discharge current, Ne/Xe/HCl mix ratio, and total discharge pressure. The discharge current is varied over the range of 10 to 60 milliamps/channel. The mix ratios are varied from 100% Ne/0% Xe to 0% Ne/100% Xe and percentages of HCl from 0% to 8%. Three total pressures are used; 4 Torr, 2 Torr, and 1 Torr.

After the gases are mixed, the discharge is first run at 4 Torr. Plots of 308 nm intensity versus current and discharge intensity versus wavelength are usually made. This discharge is then shut off, the butterfly valve opened and the total system pressure dropped to 2 Torr. The butterfly valve is then again closed and data is taken for the 2 Torr condition. The same procedure is followed for the 1 Torr condition.

Spectral measurements are produced with the monochromator scanning and operating the time base plug-in in the X-Y plotter. Wavelengths from 200 nm to 500 nm are scanned. A typical plot is shown in figure 11.

The 308 nm intensity versus discharge current plots are produced with the monochromator set at 308 nm and the X-axis position driven by the output of the high voltage isolation amplifier. The discharge current is varied by sweeping the current regulator by hand from 10 to 60 ma. A typical intensity versus current plot is shown in figure 12.

### III. Theory

#### Hollow Cathode Discharge Model

The hollow cathode model for this discussion is shown in figure 8. The negative glow is assumed to form a homogeneous cylinder of radius  $r$ . Due to the symmetry of the hollow cathode between anodes, the field along the cathode axis is assumed to equal zero at section A-A. The field then increases toward each anode and reaches a maximum at section B-B.

Total Current. The total current density crossing section B-B is  $j_g$ . No current is assumed to cross section A-A, since the field is zero. The total discharge current  $I$  is then just  $j_g$  times the area of the negative glow at section B-B or,

$$I = \pi r^2 j_g. \quad (5)$$

The cathode current density,  $j_c$ , times the cathode surface area within  $L$  also yields the total current.

$$I = 2 \pi r L j_c \quad (6)$$

Using equations 5 and 6 and solving for  $j_c$ .

$$j_c = \frac{r}{2L} j_g \quad (7)$$

Cathode Current Density. The cathode current density is made up of electrons emitted from the cathode ( $j_c^e$ ) and positive ions falling upon it ( $j_c^+$ ) or,

$$j_c = j_c^e + j_c^+ \quad (8)$$

The electrons released from the cathode are the result of positive ions and photons hitting the cathode. The electron current density at the cathode and the electron current density in the glow are related by

$$j_c^e = \gamma_1 j_c^+ + G j_g^e. \quad (9)$$



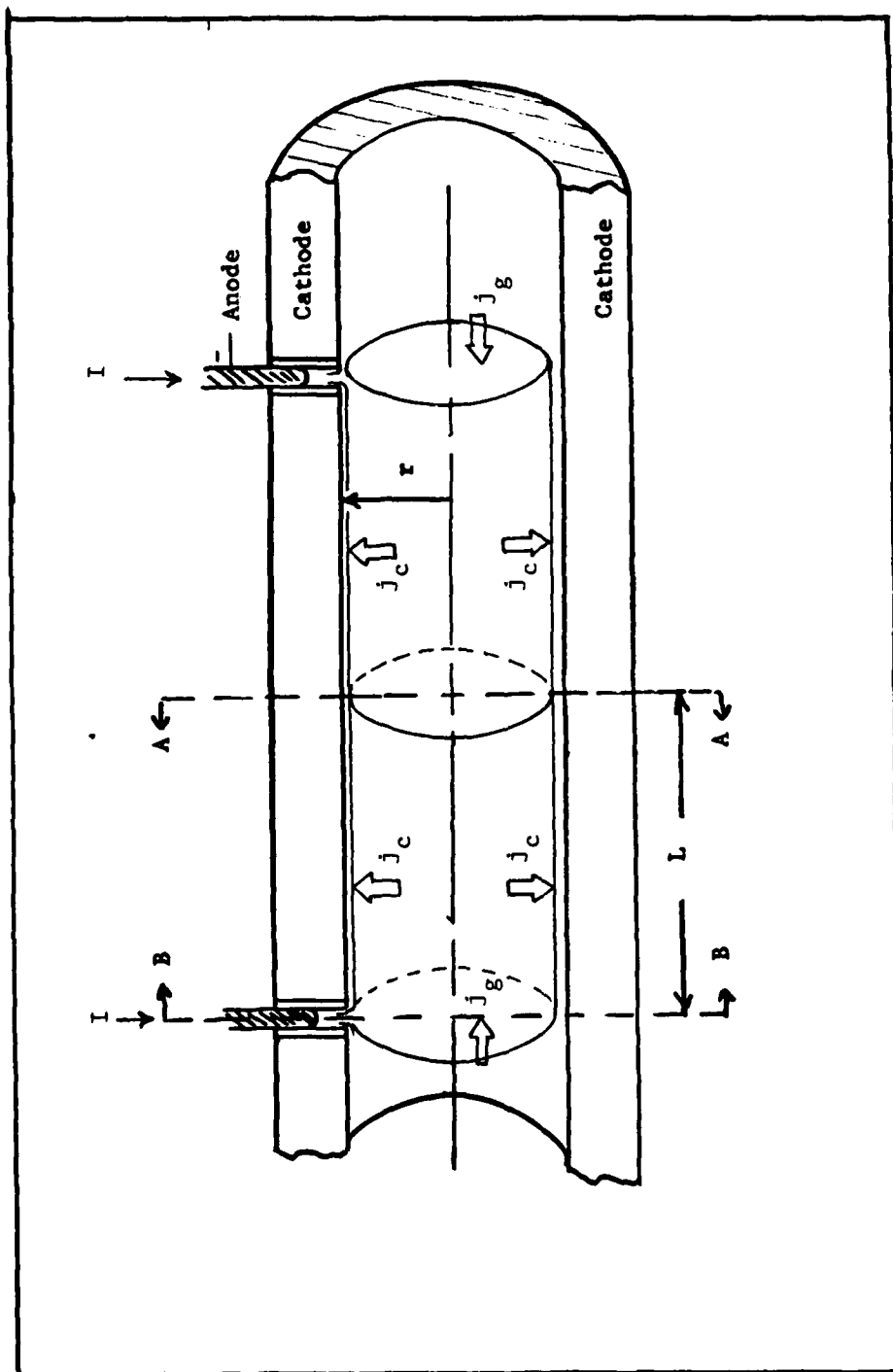


Figure 8. Hollow cathode discharge model.

G is defined by

$$G = f_g \gamma_p n_g, \quad (10)$$

where  $f_g$  is a geometric factor,  $\gamma_p$  the photo-electric yield in electrons per photon hitting the cathode, and  $n_g$  the number of energetic photons per electron in the glow.  $\gamma_i$  is the number of electrons released per positive ion hitting the cathode.

Glow Current Density. The glow current density is

$$j_g = j_g^e + j_g^- + j_g^+, \quad (11)$$

where  $j_g^e$  is the glow electron current density, and  $j_g^-$  is the glow negative ion current density, and  $j_g^+$  is the glow ion current density.

In order to simplify the equations for later manipulation, assume

$$j_g^- = \alpha j_g^e \quad (12)$$

where  $\alpha$  is a factor relating the magnitudes of  $j_g^-$  and  $j_g^e$ .

Electron Multiplication. Each high energy electron which enters the negative glow undergoes a number of inelastic collisions producing ions and electrons. If it is assumed that the average energy lost per electron/ion pair produced is  $V_a$ , then approximately  $V_c/V_a$  electron/ion pairs are produced for each high energy electron. Furthermore, this source of electrons could be viewed as a current density ( $j_s$ ) across the cylindrical surface of the glow. Then,

$$j_s = \frac{V_c}{V_a} j_c^e. \quad (13)$$

Ion Density Steady State. Since the hollow cathode is operated with a constant discharge current, the ion density within the glow is a constant. The total number of ions entering the glow plus the total number of ions created within the glow is equal to the total number of ions leaving the glow plus the total number of ions lost to recombination.

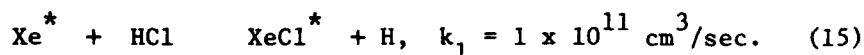
$$j_g^+ (\pi r^2) + j_g (2\pi r L) + R(\pi r^2 L) q \quad (14)$$

where R is the electron/ion recombination rate/cm<sup>3</sup>,

### Primary Reactions

The various reactions in the XeCl discharge plasma have been considered and in this thesis a reduced set of reactions is treated. This set consists of those reactions which will probably dominate on considerations of their densities and rates of reaction, when compared with reactions that may occur in parallel. Sequentially important reactions have been considered although surprises may remain as research uncovers the details of all the mechanisms. The rate constants are considered to be typical. These constants and their sources are presented in Table III.

The production XeCl\* in the hollow cathode discharge could result from four different reactions. The most likely reaction at low pressures is the "harpoon" reaction,



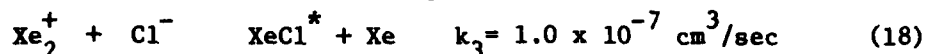
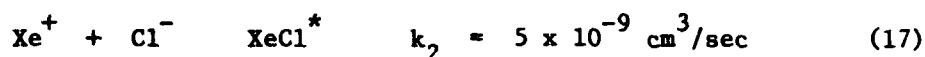
The Xe metastables can be produced by either direct electron impact excitation with the beam-like high energy cathode electrons,



or as the result of neutralization of  $\text{Xe}^+$ . A second "harpoon" reaction is also possible using the dimer  $\text{Xe}_2^*$ . This reaction is not considered here, however, since the dimer formation is a three body process and is favored only for higher pressures. Radiative decay of  $\text{Xe}_2^*$  is also more likely to occur than a collision with a HCl molecule. The process leading to the formation of  $\text{XeCl}^*$  by the harpoon reaction is commonly referred to as the neutral channel.

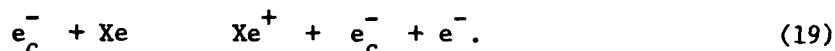
The ion channels for excimer production use either  $\text{Xe}^+$  or  $\text{Xe}_2^+$  which

combine with the  $\text{Cl}^-$  ion to form  $\text{XeCl}^*$ .

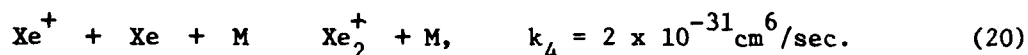


Both reactions occur at high rates due to the mutual coulombic attraction of the positive and negative ions. Equation 17 actually requires a third body to carry off excess energy and allow the ions to become bound (7: 517). The equation is given here as a two body equation to allow comparison between rates of competing reactions. Reaction constant  $k_2$  is calculated assuming a total pressure of 4 torr and independence of third body type.

As with the  $\text{Xe}^*$ , the  $\text{Xe}^+$  is formed by electron impact ionization with the beam-like high energy cathode electrons,

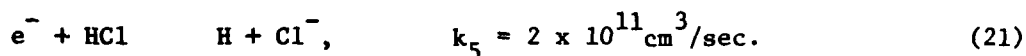


The  $\text{Xe}^+$  can then combine with another Xe in the presence of third body (M) to form the dimer ion  $\text{Xe}_2^+$ ,



The rate constant used here is for the third body being Xe; it is not significantly different if the third body is Ne. Even though the concentration of  $\text{Xe}_2^+$  is expected to be low, it is included here since its recombination rate with  $\text{Cl}^-$  is high.

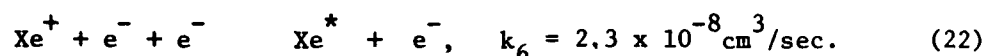
The negative ions  $\text{Cl}^-$  are formed by the dissociative attachment of electrons with HCl,



This rate constant includes the increased cross section effect for higher vibration levels ( $v = 1, 2$ ) of HCl. The rate constants were taken from reference 8 for a He/Xe/HCl mix of 95/5/0.2, assuming an E/N of Td.

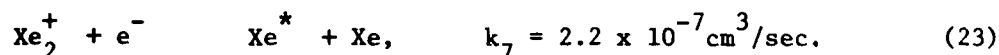
Including the additional vibration levels approximately doubles the rate constant over that for HCl ( $v = 0$ ).

There are a number of reactions which tend to reduce the concentrations of the reactants required for  $\text{XeCl}^*$  formation. Direct electron recombination with the  $\text{Xe}^+$  occurs,

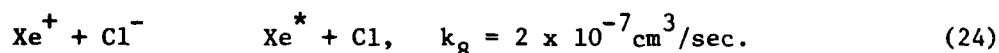


where  $k_6$  is calculated as a two body rate constant requiring just  $\text{Xe}^+$  and one  $e^-$  and assumes electron density of  $10^{12}/\text{cm}^3$  and an energy of  $700^\circ\text{K}$ .

The  $\text{Xe}_2^+$  dimer ion is neutralized in a similar reaction,



In direct competition with the ion channel is the mutual neutralization of  $\text{Xe}^+$  and  $\text{Cl}^-$ ,



Note that all of the above reactions also help to increase the  $\text{Xe}^*$  concentration. Kolts et al (Ref 5) have shown that the harpoon reaction (eqn. 15) is not the most probable outcome when  $\text{Xe}^*$  and HCl collide. The more probable result is,

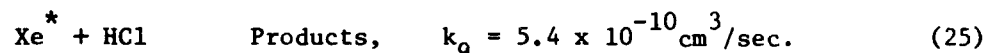


Figure 9 summarizes the main energy pathways for  $\text{XeCl}^*$  exciplex formation via three body recombination and harpoon reactions.

#### Rate Equations

The above reactions are used in the following section to write the rate equations for steady state discharge conditions. These equations are then solved for the various species number densities. Each species will be considered in turn.

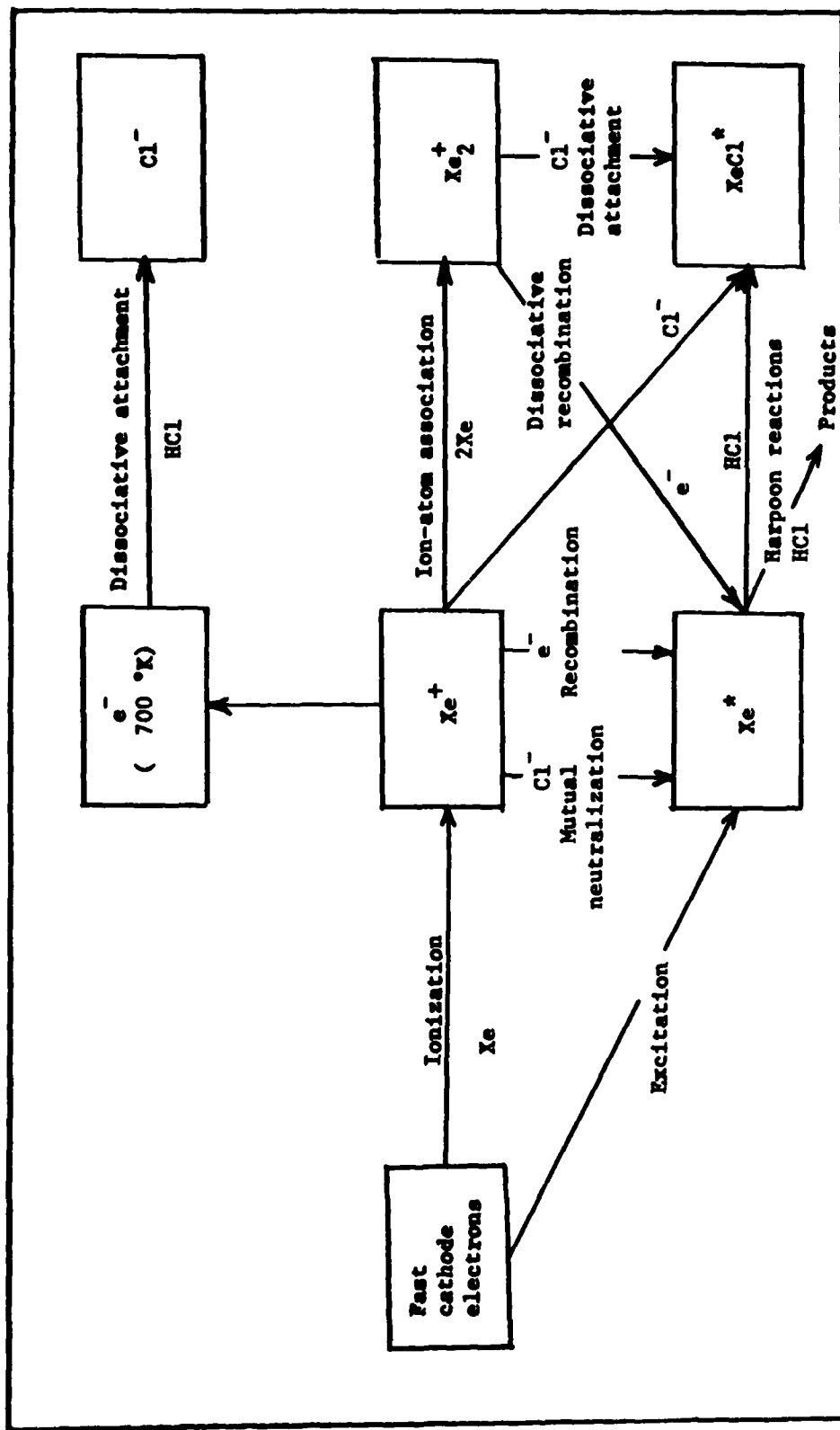


Figure 9. Dominant mechanisms for production of  $\text{XeCl}^*$  in a hollow cathode two-component rare-gas-halide system at pressures of 1-4 torr.

Table III

Summary of Primary Reactions. In Hollow Cathode Discharge Containing  
Ne, Xe, HCl.

| Reaction   | Rate Constant   | Reference |
|--|---|-----------|
| 1. $\text{Xe}^* + \text{HCl} \rightarrow \text{XeCl}^* + \text{H}$     | $k_1 = 1 \times 10^{11} \text{ cm}^3/\text{sec}$      | 5         |
| 2. $\text{Xe}^+ + \text{Cl}^- \rightarrow \text{XeCl}^*$               | a, b $k_2 = 5 \times 10^{-9} \text{ cm}^3/\text{sec}$ | 10        |
| 3. $\text{Xe}_2^+ + \text{Cl}^- \rightarrow \text{XeCl}^* + \text{Xe}$ | c $k_3 = 1 \times 10^{-7} \text{ cm}^3/\text{sec}$    | 7         |
| 4. $\text{Xe}^+ + \text{Xe} \rightarrow \text{Xe}_2^+$                 | a $k_4 = 2.8 \times 10^{-14} \text{ cm}^3/\text{sec}$ | 11        |
| 5. $e^- + \text{HCl} \rightarrow \text{H} + \text{Cl}^-$               | $k_5 = 2 \times 10^{11} \text{ cm}^3/\text{sec}$      | 8         |
| 6. $\text{Xe}^+ + e^- \rightarrow \text{Xe}^*$                         | $k_6 = 2.3 \times 10^{-8} \text{ cm}^3/\text{sec}$    | 12        |
| 7. $\text{Xe}_2^+ + e^- \rightarrow \text{Xe}^* + \text{Xe}$           | $k_7 = 2.2 \times 10^{-7} \text{ cm}^3/\text{sec}$    | 11        |
| 8. $\text{Xe}^+ + \text{Cl}^- \rightarrow \text{Xe}^* + \text{Cl}$     | c $k_8 = 2. \times 10^{-7} \text{ cm}^3/\text{sec}$   | 7         |
| 9. $\text{Xe}^* + \text{HCl} \rightarrow \text{products}$              | $k_9 = 5.4 \times 10^{-10} \text{ cm}^3/\text{sec}$   | 5         |
| 10. $e_c^- + \text{Xe} \rightarrow \text{Xe}^+ + e_c^- + e^-$          |   |           |
| 11. $e_c^- + \text{Xe}^* \rightarrow \text{Xe}^* + e_c^-$              |   |           |

a Three body reaction calculated for 4 Torr total pressure.  
b Estimate from KrF  
c Estimate from ArF

$\text{Xe}^+$ . The primary source for the xenon ions is from electron impact ionization (equation 19). This source is directly related to the source current density ( $j_s$ ). The total ionization rate in the volume ( $\pi r^2 L$ ) is  $2\pi r L j_s$ . The ionization rate per unit volume is then  $\frac{2}{r} j_s$ . In a similar manner the loss of ions to the negative glow due to the cathode ion current is  $\frac{2}{r} j_c^+$ .

$$\begin{aligned} \frac{d[\text{Xe}^+]}{dt} = & \frac{2}{r} j_s - \frac{2}{r} j_c^+ - k_2 [\text{Xe}^+][\text{Xe}] - k_6 [\text{Xe}^+][e^-] \\ & - k_8 [\text{Xe}^+][\text{Cl}^-], \end{aligned} \quad (26)$$

where  $k_4$  has been defined as a effective two body rate at 4 torr.

In steady state,

$$[\text{Xe}^+] = \frac{\frac{2}{r} (j_s - j_c^+)}{(k_2 + k_8) [\text{Cl}^-] + k_4 [\text{Xe}] + k_6 [e^-]} \quad (27)$$

Under normal conditions with low concentrations of HCl, the electron-ion recombination term ( $k_6 \text{Xe}$ ) will dominate the other terms in the denominator.

$\text{Xe}_2^+$ . The  $\text{Xe}_2^+$  dimer ion is produced by the three body ion-atom association. The losses are by dissociative recombination and combining with  $\text{Cl}^-$  to form  $\text{XeCl}^+$ ,

$$\frac{d[\text{Xe}_2^+]}{dt} = k_4 [\text{Xe}^+][\text{Xe}] - k_7 [\text{Xe}_2^+][e^-] - k_3 [\text{Xe}_2^+][\text{Cl}^-]. \quad (28)$$

In steady state,

$$[\text{Xe}_2^+] = \frac{k_4 [\text{Xe}^+][\text{Xe}]}{k_7 [e^-] + k_3 [\text{Cl}^-]} \quad (29)$$

Since  $k_7 \approx k_3$  and assuming  $[\text{Cl}^-] \ll [e^-]$ , the dissociative recombination term ( $k_7 [e^-]$ ) in the denominator will dominate. Also, since the plasma is essentially neutral ( $[e^-] \approx [\text{Xe}^+]$ ), it is easily seen that,



$$[\text{Xe}_2^+] \approx \frac{k_4}{k_7} [\text{Xe}] \quad (30)$$

Cl<sup>-</sup>. The Cl<sup>-</sup> ion is created by dissociative attachment of electrons with HCl. Cl<sup>-</sup> is lost by forming the XeCl<sup>\*</sup> excimer with Xe<sup>+</sup> and Xe<sub>2</sub><sup>+</sup> and by neutralization with Xe<sup>+</sup>,

$$\frac{d[\text{Cl}^-]}{dt} = k_5[\text{HCl}][e^-] - k_2[\text{Xe}^+][\text{Cl}^-] - k_3[\text{Xe}_2^+][\text{Cl}^-] - k_8[\text{Xe}^+][\text{Cl}^-]. \quad (31)$$

In steady state,

$$\text{Cl}^- = \frac{k_5[\text{HCl}][e^-]}{(k_2 + k_8)[\text{Xe}^+] + k_3[\text{Xe}_2^+]}. \quad (32)$$

The  $k_8[\text{Xe}^+]$  term in the denominator will dominate since  $k_8 \approx k_3$  and  $[\text{Xe}^+] \gg [\text{Xe}_2^+]$ .

Xe<sup>\*</sup>. The formation of the Xe<sup>\*</sup> is primarily due to direct impact excitation by the cathode electrons and, like Xe<sup>+</sup>, is equal to  $\frac{2}{r} j_s$ . Small amounts of Xe<sup>\*</sup> are also formed by neutralization of Xe<sup>+</sup> and Xe<sub>2</sub><sup>+</sup>. The Xe<sup>\*</sup> is quenched by the harpoon reaction with HCl.

$$\begin{aligned} \frac{d[\text{Xe}^*]}{dt} = & \frac{2}{r} j_s + k_6[\text{Xe}^+][e^-] + k_7[\text{Xe}_2^+][e^-] + k_8[\text{Xe}^+][\text{Cl}^-] \\ & - k_1[\text{Xe}^*][\text{HCl}] - k_9[\text{Xe}^*][\text{HCl}] \end{aligned} \quad (33)$$

In steady state,

$$\text{Xe}^* = \frac{\frac{2}{r} j_s + k_6[\text{Xe}^+][e^-] + k_7[\text{Xe}_2^+][e^-] + k_8[\text{Xe}^+][\text{Cl}^-]}{(k_1 + k_9) [\text{HCl}]} \quad (34)$$

XeCl<sup>\*</sup>. Finally the XeCl<sup>\*</sup> rate equation is considered. The spontaneous life time ( $\tau$ ) is taken to be 11 ns,

$$\frac{d[\text{XeCl}^*]}{dt} = k_1[\text{Xe}^*][\text{HCl}] + k_2[\text{Xe}^+][\text{Cl}^-] + k_3[\text{Xe}_2^+][\text{Cl}^-] - \frac{1}{\tau}[\text{XeCl}^*]. \quad (35)$$

In steady state,

$$[\text{XeCl}^*] = \tau k_1 [\text{Xe}^*][\text{HCl}] + \tau k_2 [\text{Xe}^+][\text{Cl}^-] + \tau k_3 [\text{Xe}_2^+][\text{Cl}^-]. \quad (36)$$

Each of the terms on the right is associated with one of the three major excimer formation reactions. The first term is from the neutral channel harpoon reaction. The other two terms are from the ion channel and are the result of the ion-ion recombination of  $\text{Cl}^-$  with  $\text{Xe}^+$  and  $\text{Xe}_2^+$  respectively.

All of the above reactions appear to be the major contributions to  $\text{XeCl}^*$  formation. The most apparent omission from this list is reactions involving the buffer gas Ne. This omission is justified since the cross section for ionization of Ne is about one eighth that of Xe for high energy electrons and the concentration of Ne never exceeds eight times that of Xe. Also, even under this worst case condition, it is assumed that the Ne ions and metastables formed in the discharge eventually ionize or excite the Xe and thus give the same result as if the Xe were excited directly by the high energy electrons. Also considered was the quenching of the  $\text{XeCl}^*$  by Xe and HCl. Finn et. al. (REF 9: 790) report these rate constants to be of the order of  $3.2 \times 10^{-11} \text{ cm}^3/\text{sec}$  and  $1.4 \times 10^{-9} \text{ cm}^3/\text{sec}$  respectively. For 8% HCl at 4 torr the effective HCl quenching time constant would be  $6 \times 10^{-8} \text{ sec}$ . This is somewhat slower than the 11 ns spontaneous lifetime of  $\text{XeCl}^*$  so it may come into consideration for high HCl concentrations.

#### IV. Analysis and Discussion of Results

##### XeCl<sup>\*</sup> Spectral Characteristics

Figure 10 shows the potential curves for XeCl. The three main spectroscopic transitions are B-X, C-A, and D-X. The B-A transition competes with the B-X transition for the heavier halogens. The XeCl B-A transition, which is quite weak, slightly augments the emission intensity in the wavelength region of the C-A transition (Ref 5: 1249). Table IV shows the calculated and experimental emission energies, wavelengths, and lifetimes for these transitions and the D-A transition.

A typical XeCl<sup>\*</sup> emission spectrum obtained in the hollow cathode discharge is shown in figure 11. The strongest B-X emission peaks at about 308 nm and is degraded to the ultraviolet. The D-X emission is centered at 235 nm. The broad C-A emission is seen as a constant amplitude spectrum from about 320 nm to past 390 nm. Both the D-A and B-A emissions are too weak and broad to be distinguished from the other stronger emissions. Nearly all of the atomic lines seen from 460 to 500 nm are transitions of neutral Xe to the Xe (6s, <sup>3</sup>P<sub>2</sub>) metastable.

##### Dominant Reactions

Electron Density and Temperature. The electron density and temperature is based upon the measurements of Gerstenberger et. al. (Ref 13: 829) who used a copper hollow cathode with a 0.3 cm diameter. Their measurements, which were made using spectroscopic techniques, show both electron temperature and density to be linear functions of discharge current density. This result indicates that the hollow cathode discharge studied by them is diffusion dominated and that two- and three-body recombination may be ignored, at least to the first order. In order to get an estimate on the

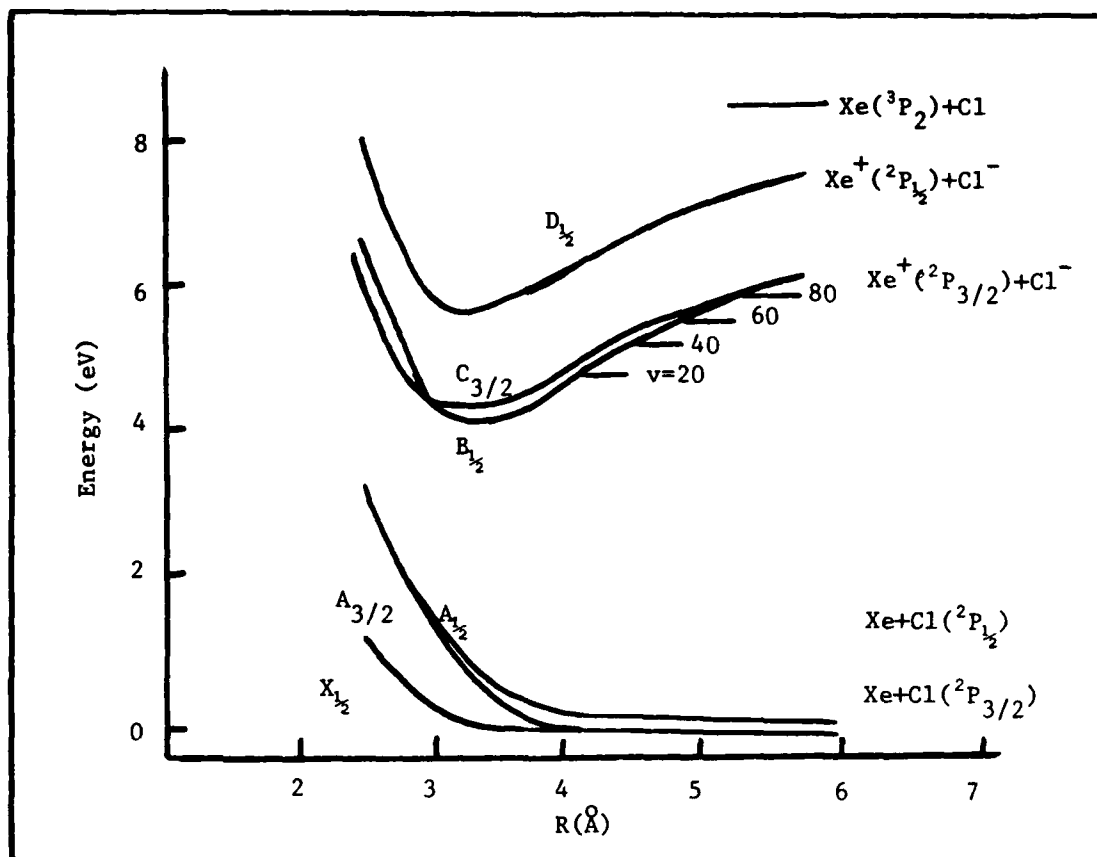


Figure 10. Calculated potential curves for XeCl (Ref 18: 2213).

Table IV

Calculated and experimental emission energies ( $\Delta E$ ), wavelengths ( $\lambda$ ), and life times ( $\tau$ ) for ionic-covalent transitions in XeCl (Ref 18: 2217).

| Strongest emission<br>bands | $\Delta E$ (ev) |              | $\lambda$ (nm) |              | $\tau$ (ns) |
|-----------------------------|-----------------|--------------|----------------|--------------|-------------|
|                             | Calculated      | Experimental | Calculated     | Experimental |             |
| 1. $B_{1/2} - X_{1/2}$      | 4.20            | 4.03         | 295            | 308          | 11          |
| 2. $D_{1/2} - X_{1/2}$      | 5.53            | 5.25         | 224            | 235.8        | 9.6         |
| 3. $C_{3/2} - A_{3/2}$      | 3.76            |              | 330            | 320-360      | 120         |
| 4. $D_{1/2} - A_{1/2}$      | 5.13            |              | 242            |              | 180         |
| 5. $B_{1/2} - A_{1/2}$      | 3.83            |              | 324            |              | 140         |

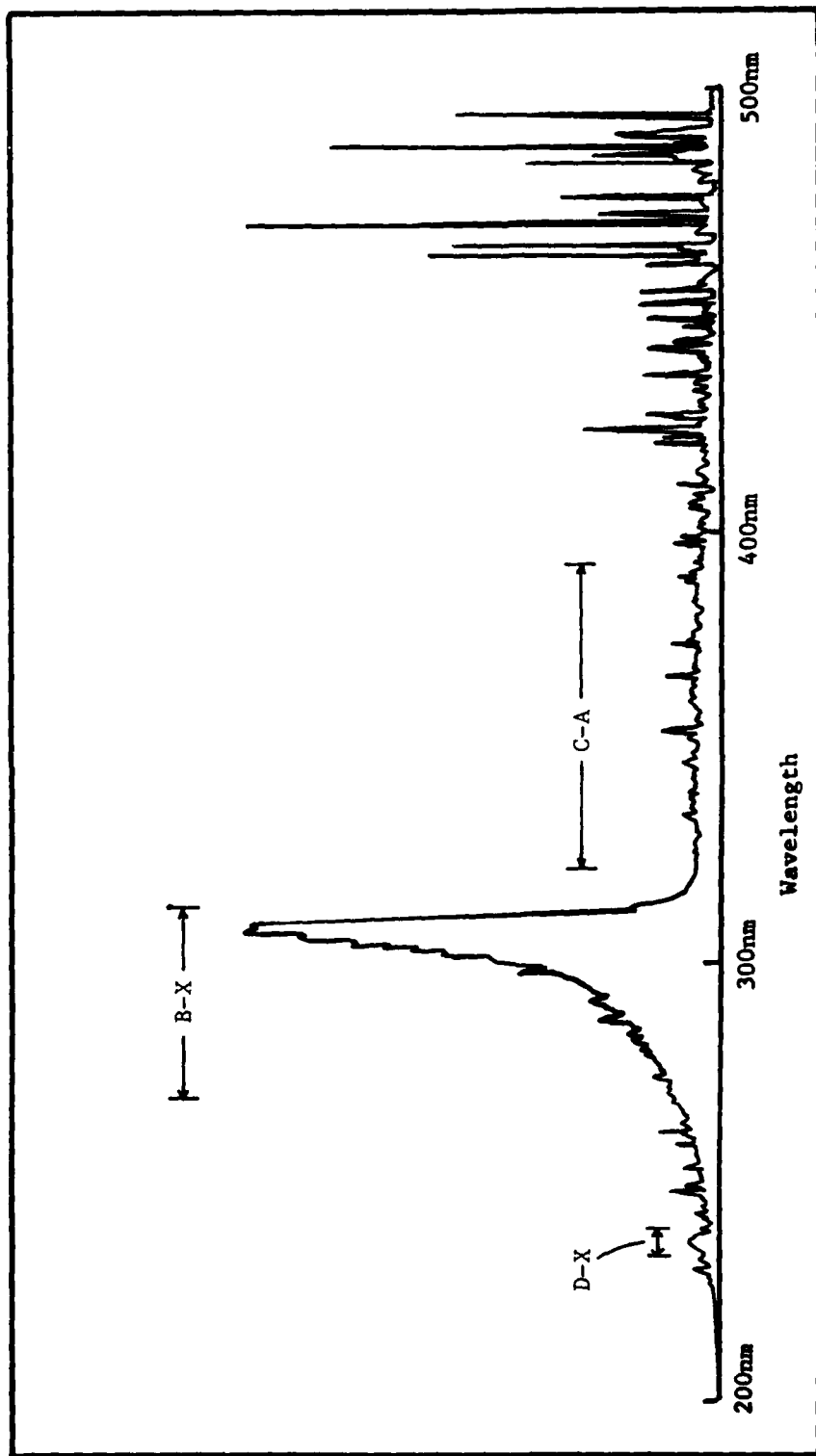


Figure 11. XeCl\* spectrum 200 - 500 nm.

electron temperature and density it is assumed that Gerstenberger's hollow cathode discharge and the  $\text{XeCl}^*$  hollow cathode discharge are equivalent. For the latter discharge a 200 ma current results in a current density of  $4 \text{ ma/cm}^2$ . Using Gerstenberger's data and this current density the electron temperature and density are found to be  $700^\circ\text{K}$  and  $10^{12}/\text{cm}^3$  respectively. It is further assumed that the electron density is not affected by the  $\text{Cl}^-$  since the current is held constant and is dominated by electron diffusion. Based upon analysis performed by Persson (Ref 14: 3086-3087) it can be shown that in a diffusion dominated discharge, the low energy electron density can be written as

$$[e^-] = \frac{S}{2D_A} \left[ \left(\frac{d}{2}\right)^2 - x^2 \right] \quad (38)$$

where  $S$  is the source of the low energy electrons,  $D_A$  is the ambipolar diffusion coefficient of electrons in the rare gas, and  $d$  is the length of the discharge region centered at  $x = 0$ . All discussions in this thesis have assumed this distribution to be constant with respect to  $x$ .

Discharge Conditions with Trace HCl. In order to get a grasp of the component densities, the approach is to first assume only a trace amount of HCl and thus  $\text{Cl}^-$ . Once the baseline densities are determined it is then possible to return to the original equations to establish when they are perturbed by additional HCl. The following densities are assumed:  $[e^-] = 10^{12}/\text{cm}^3$ , total pressure = 4 torr,  $[\text{Xe}] = 1.4 \times 10^{16}/\text{cm}^3$  (10% Xe) and  $\frac{2}{r} j_s = 7 \times 10^{16}$  ionizations/ $\text{cm}^2$  sec. With these assumptions the following equations result:

$$[\text{Xe}^+] = [\text{Cl}^-] + [e^-] \approx [e^-] = 10^{12}/\text{cm}^3 \quad (\text{plasma neutrality}) \quad (39)$$

$$[\text{Xe}_2^+] = \frac{k_4[\text{Xe}^+][\text{Xe}]}{k_7[e^-] + k_3[\text{Cl}^-]} \approx \frac{k_4[\text{Xe}]}{k_7} \approx 1.3 \times 10^7/\text{cm}^3 \quad (40)$$

$$[Cl^-] = \frac{k_5 [HCl][e^-]}{(k_2 + k_8) [Xe^+] + k_3 [Xe_2^+]} \quad \frac{k_5}{k_8} [HCl] = 1 \times 10^{-4} [HCl] \quad (41)$$

$$[Xe^*] = \frac{\frac{2}{r} j_s + k_6 [Xe^+][e^-] + k_7 [Xe_2^+][e^-] + k_8 [Xe^+][Cl^-]}{(k_1 + k_9) [HCl]} \\ = \frac{\frac{2}{r} j_s}{k_9 [HCl]} = \frac{1.3 \times 10^{26}}{[HCl]} \quad (42)$$

$$\frac{XeCl^*}{\tau} = k_1 [Xe^*][HCl] + k_2 [Xe^+][Cl^-] + k_3 [Xe_2^+][Cl^-] \\ = 1.3 \times 10^{15} + 0.5x [HCl] + 1.3 \times 10^{-4} [HCl] \quad (43)$$

Equation 43 shows two important results. The first result is that the production of  $XeCl^*$  is independent of HCl concentration when considering only the neutral channel. This effect is the result of HCl quenching the  $Xe^*$  at the same rate as it adds to the  $XeCl^*$ . Only for very small concentrations of HCl in which the quenching of Xe metastables is dominated by some other process, collisions with the walls for example, will the  $XeCl^*$  concentration become proportional to HCl concentration. The crossover point for this process could not be measured for this thesis experiment, however, since the residual HCl within the discharge tube was too large.

The second result of equation 43 is that the rate of formation of  $XeCl^*$  using  $Xe_2^+$  is significantly less than the rate of formation due to direct ion-ion recombination at these pressures. Furthermore, for HCl concentrations greater than  $1.4 \times 10^{15}/cm^3$  (1% HCl at 4 torr),  $XeCl^*$  is primarily formed by the combination of  $Xe^+$  and  $Cl^-$  (equation 17). Assuming sufficient HCl concentrations the following rate equation for  $XeCl^*$  spontaneous emission results,

$$\frac{XeCl^*}{\tau} = k_2 [Cl^-][Xe^+] = \frac{k_2 k_5}{k_8} [HCl][Xe] j_c. \quad (44)$$

The experimental data should thus verify this equation by showing that the  $\text{XeCl}^*$  emissions are proportional to Xe and HCl concentrations as well as discharge current.

Discharge Voltage vs  $[\text{Cl}^-]$ . Throughout the experiment it is noted that as additional amounts of HCl are added, with all other controlled variables remaining constant, the discharge voltage increases. The additional HCl removes electrons by dissociative attachment to form  $\text{Cl}^-$ . The additional  $\text{Cl}^-$  in turn, tends to reduce the  $\text{Xe}^+$  concentration by ion-ion neutralization. In order for the discharge to maintain a constant current, the losses in the xenon ion and electron concentrations must be made up for by an increased ionization rate. The discharge voltage, which is predominately  $V_c$ , thus increases. Quantitatively this process can be seen in the following two equations,

$$[\text{Xe}^+] = [\text{Cl}^-] + [\text{e}^-] \quad (\text{charge neutrality}), \quad (39)$$

$$[\text{Xe}^+] = \frac{\frac{2}{r} \left( \frac{V_c}{V_a} \gamma_1 - 1 \right) \frac{j_c}{1 + \gamma_1}}{k_8 [\text{Cl}^-] + k_6 [\text{e}^-]}, \quad (45)$$

where equation 45 is a simplification of equation 27 showing only the dominant parameters in the denominator and giving  $j_s$  and  $j_c^+$  in terms of ionization rate ( $V_c/V_a$ ), cathode current density ( $j_c$ ), and the number of electrons released per positive ion hitting the cathode ( $\gamma_1$ ). Throughout this discussion it is assumed that the electron concentration is constant. This is possible since the fields within the glow are very small and the current density, which is constant, is due primarily to electron diffusion out the end of the glow to the anode. For  $[\text{Cl}^-] \ll [\text{e}^-]$  the  $[\text{Xe}^+]$  is constant and it is easily shown that,



$$\frac{V_{c\Delta}}{V_a} = \frac{k_8[Xe^+][Cl^-]}{\frac{2}{r} j_c},$$

where  $V_{c\Delta}$  is the change in discharge voltage due to the addition of HCl.

The change in discharge voltage is thus proportional to Cl ion concentration for  $[Cl^-] \ll [e^-]$ .

### Results

Equation 44 summarizes the results of theoretical analysis.

$$\frac{XeCl}{\tau}^* \propto \frac{k_2 k_5}{k_8} [HCl][Xe] j_c \quad (44)$$

For this analysis the spontaneous emission is only a soft function of  $[Xe]$  since it is assumed that  $Xe^+$  is the only ionized species in the discharge and few electrons are lost to ionization and recombination with the buffer gas. Although equation 44 was derived assuming low  $Cl^-$  concentration, it can be shown by assuming  $[Xe^+] = [Cl^-]$  and using equation 33 to solve for  $[Cl^-]$ , that it is equally valid for high  $Cl^-$  concentrations.

308 nm Intensity vs Current. Figure 12 shows a representative plot of the variation of the rate of spontaneous emission with discharge current. The procedure used for taking this measurement is described in section III, Experimental Program, under the heading entitled Intensity Measurements. Figure 12, which is representative of nearly all measurements made for different mixes and pressures, demonstrates that the 308 nm intensity is proportional to discharge current in the range of 10 to 60 milliamperes per channel. This result is in agreement with equation 44 developed analytically.

Although figure 12 shows a fairly well behaved condition, there were cases that were not so well behaved. Probably the biggest contributor to nonreproducible results was discharge temperature. If the discharge current was held high too long the hollow cathode would become warmer and change

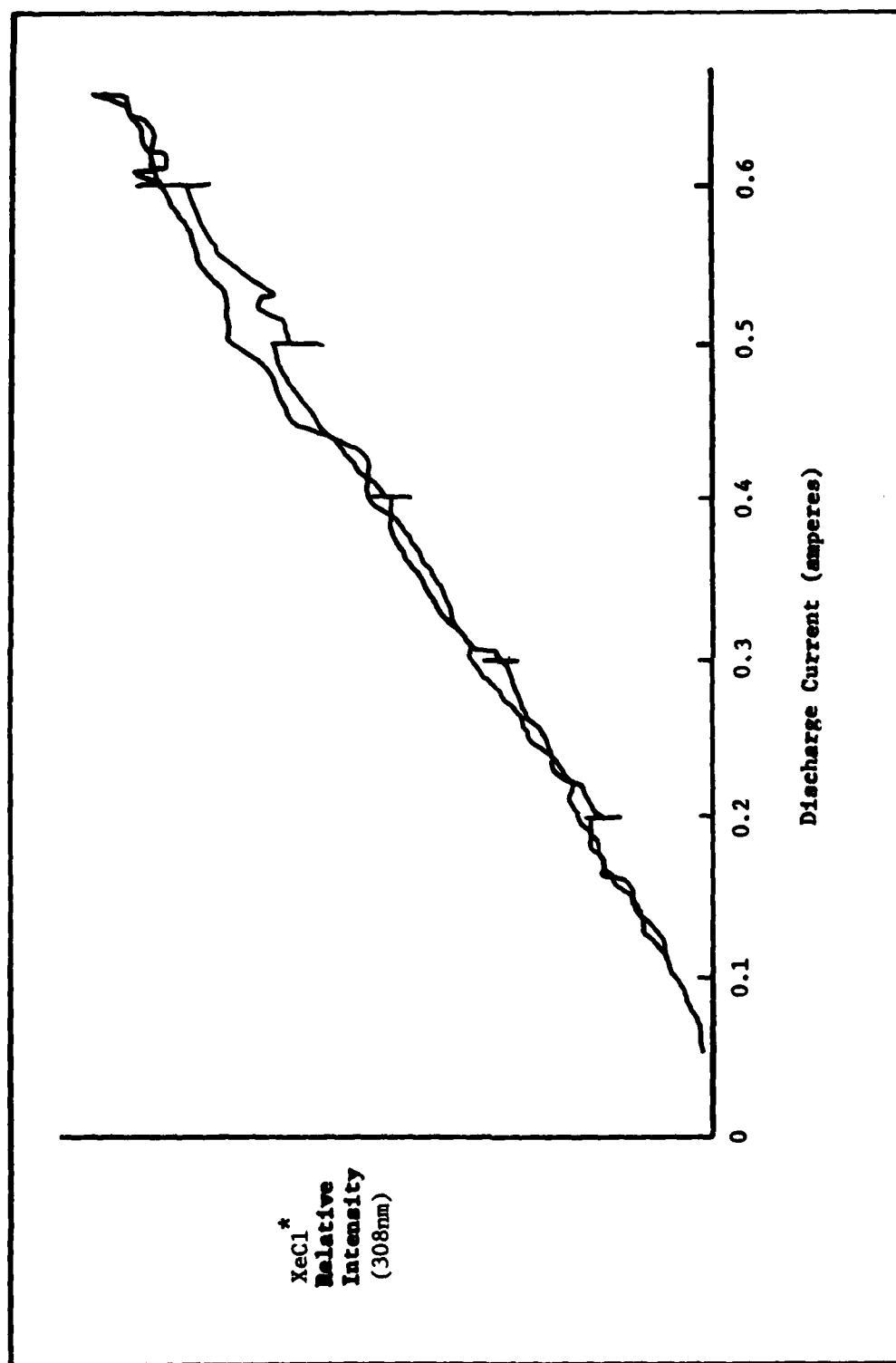


Figure 12. Relative XeCl\* output vs total discharge current.

the discharge voltage. For this reason the intensity vs current sweeps were made as quickly as possible. Even with this precaution, however, the excimer emission intensity might fluctuate as much as 10 to 20% during a scan.

308 nm Intensity vs HCl Concentration. A large number of Ne/Xe/HCl mixes were investigated from 100% Ne to 100% Xe with 0 to 8% HCl added. Many of these mixes have questionable results, however, due to an apparent leak in one or more of the hollow cathode anodes. The majority of the good measurements were obtained for Ne/Xe mixes at ratios of 5/1 and 1/1. A second problem is related to the measurement of HCl concentration. After the hollow cathode is sealed off with its chosen mix of gases and the discharge is initiated, the excimer emission will usually decrease. This decrease is attributed to the loss of Cl to the walls of the hollow cathode or possibly a reaction with the copper gaskets used for connecting the tube to the vacuum system. Whatever the loss mechanism, it is not possible to determine what the HCl concentration is after several minutes of discharge time, based solely upon the initial conditions. It is for this reason that the theory relating discharge voltage to  $\text{Cl}^-$  concentration was developed earlier in this thesis.

Figures 13 and 14 show how the XeCl excimer intensity varies with discharge voltage for two different mix ratios of Ne and Xe. These plots demonstrate that the excimer emission is a linear function of discharge voltage when the discharge current is held constant and the concentration of HCl is varied. From equations 41 and 46 ( $[\text{Xe}^+]$  assumed constant) the change in discharge voltage due to the addition of HCl is simply proportional to the amount of HCl added. Figures 13 and 14 thus show that the  $\text{XeCl}^*$  output in the hollow cathode is a linear function of HCl concentration as predicted by equation 44.

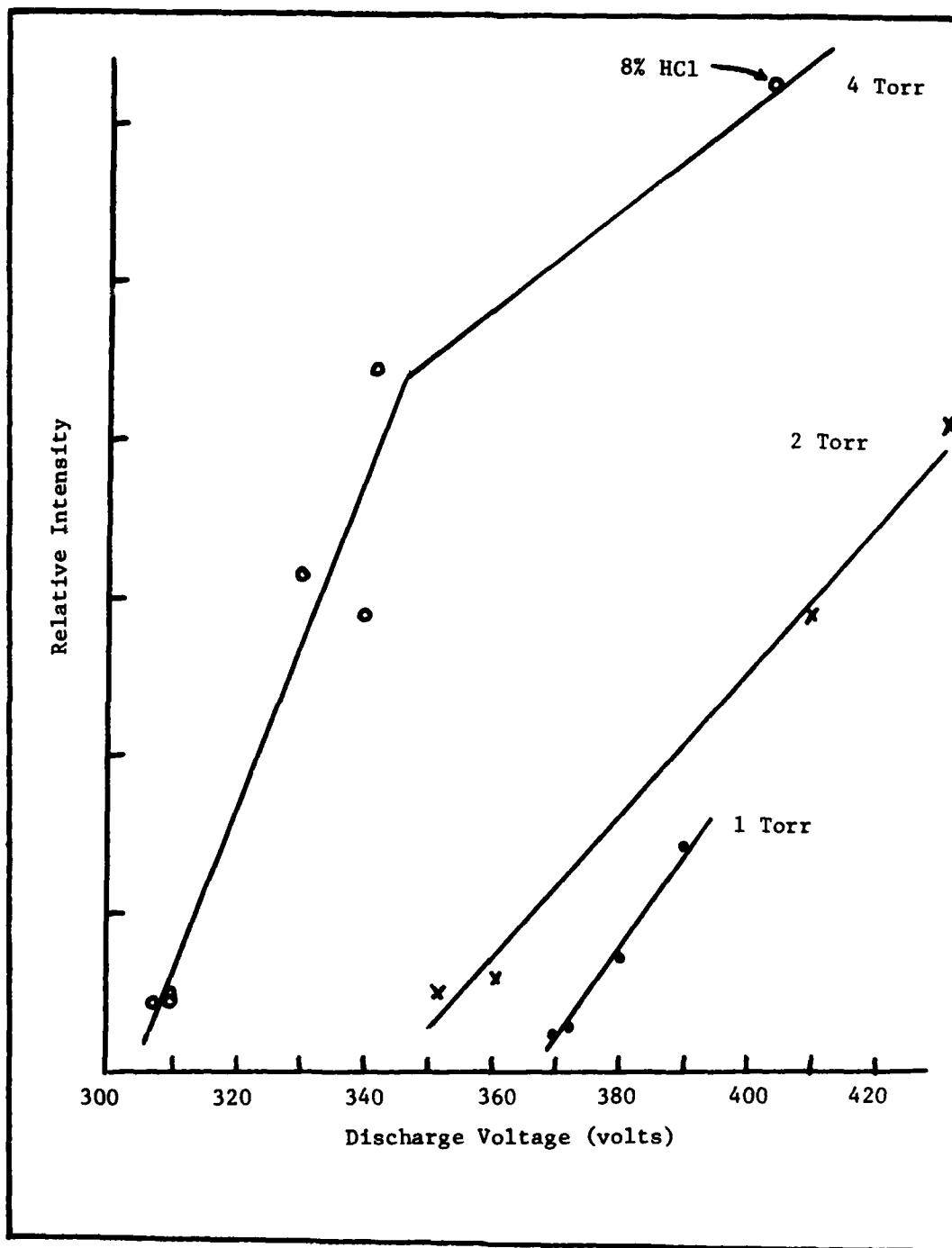


Figure 13. Relative XeCl\* output vs discharge voltage in hollow cathode with Ne/Xe = 1/1, total pressure = 1, 2, and 4 torr, discharge current = 20 ma per channel, and varying amounts of HCl.

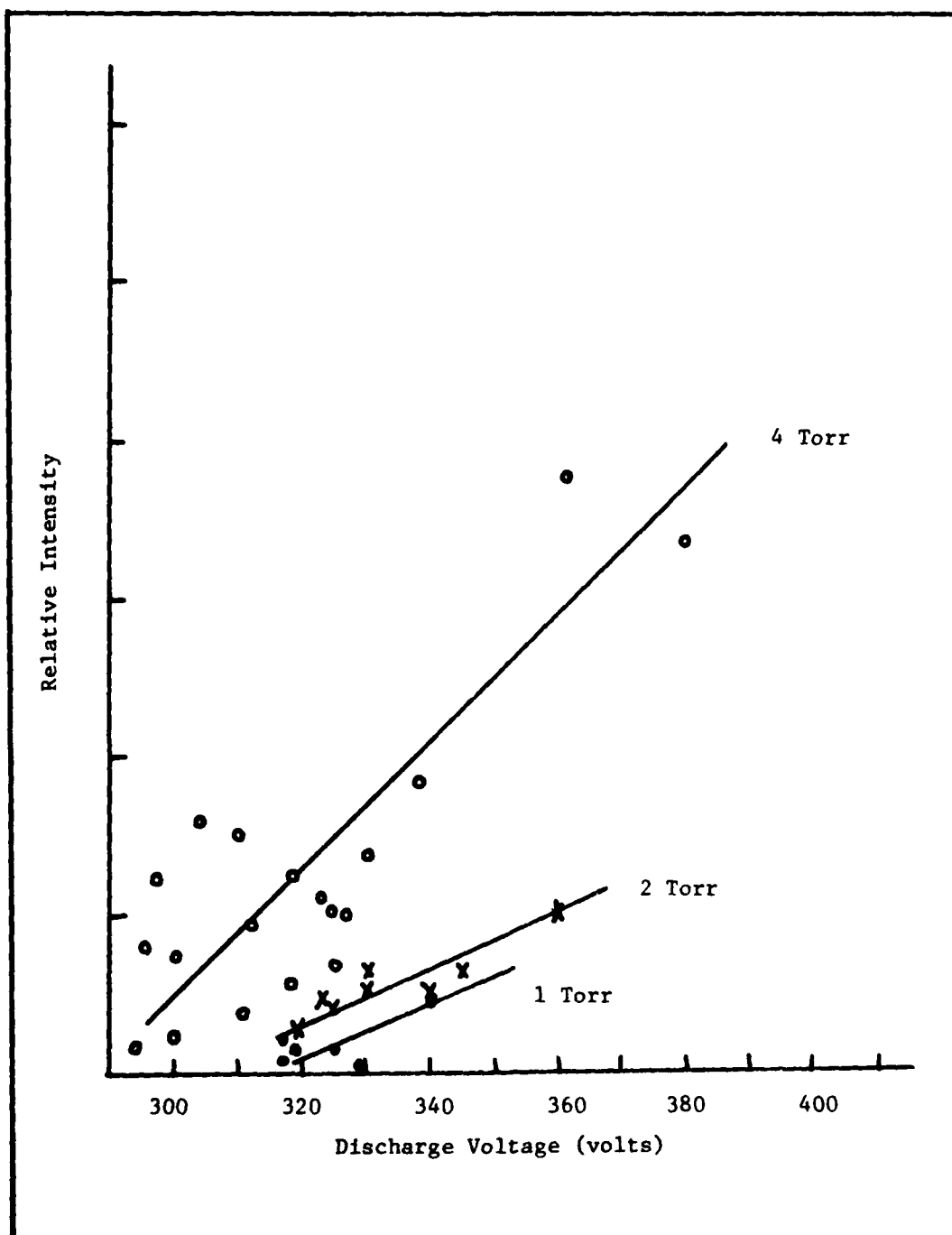


Figure 14. Relative  $\text{XeCl}^*$  output vs discharge voltage in hollow cathode with  $\text{Ne/Xe} = 5/1$ , total pressure = 1, 2, and 4 torr, discharge current = 20 ma per channel, and varying amounts of  $\text{HCl}$ .

Additional information may be gained by considering the slopes of the lines in figures 13 and 14. If equations 44 and 46 are used to solve for the slope we find that,

$$\text{slope} = \frac{[\text{XeCl}^*]}{V_{c\Delta}} = \frac{k_2}{V_a k_8 \frac{2}{r} j_c} \quad (47)$$

The increase in the slope when going from 2 torr to 4 torr is attributed to an increase in  $k_2$ , since  $k_2$  is the rate constant for a 3-body reaction, and is proportional to pressure. In both figures the slope approximately doubles for a doubling in the pressure. The fact that the slope does not change when going from 2 to 1 torr may indicate that 2 torr is the low pressure limit where  $k_2$  becomes essentially a two-body rate constant.

Equation 47 may also be applied when explaining the difference in slopes when comparing figure 13 with figure 14. Note that the line slopes decrease by about a factor of two when going from a Ne/Xe ratio of 1/1 to 5/1. This change is due to an increased amount of energy lost per ionizing collision ( $V_a$ ) for the gas mixtures containing more neon.

One reaction which was considered but not included in the rate equations is the quenching of  $\text{XeCl}^*$  with  $\text{HCl}$ . It was calculated that this reaction would not become significant except for mixes containing 8%  $\text{HCl}$  at 4 torr. The roll-off on the 4 torr curve in figure 13 is a manifestation of this quenching process, since the highest intensity point is for an 8%  $\text{HCl}$  mix.

One of the problems encountered when trying to measure discharge characteristics, in particular discharge voltage, was the effect of hollow cathode heating. The warmer the cathode surface, the lower the discharge voltage became. The effect is caused by an increase in electron

emission efficiency ( $\gamma_i$ ) with increasing temperature. As the emission efficiency increases, the required ionizations per electron decreases, and the required discharge voltage drops. It is for this reason that the data for the 4 torr condition in figure 14 is so scattered. To correct this problem for data taken later in the experiment, data is taken only after the discharge is allowed to stabilize at 20 ma per channel.

308 nm Intensity vs Xe Concentration. Initial analysis of the hollow cathode anticipated that the  $\text{Xe}^+$  concentration would be relatively independent of buffer gas concentration. This was based upon the assumption that the higher energy buffer gas ions and metastables would eventually ionize the Xe by charge exchange or harpoon reactions. Figure 15, however, shows this not to be the case. For mixes containing less than 50% Xe, the  $\text{XeCl}^*$  intensity (which is proportional to  $\text{Xe}^+$  concentration by equation 44) is linearly related to Xe concentration. This result can be explained by recalling that the hollow cathode discharge is diffusion dominated. Unlike a normal glow discharge, most Ne ions created are quickly swept out of the negative glow of the hollow cathode discharge before they can react with the Xe.

Note that using helium instead of neon for a buffer gas figure results in a slight increase in  $\text{XeCl}^*$  output. This is due to a lower ionization cross section of He and thus an increase in Xe ions created.

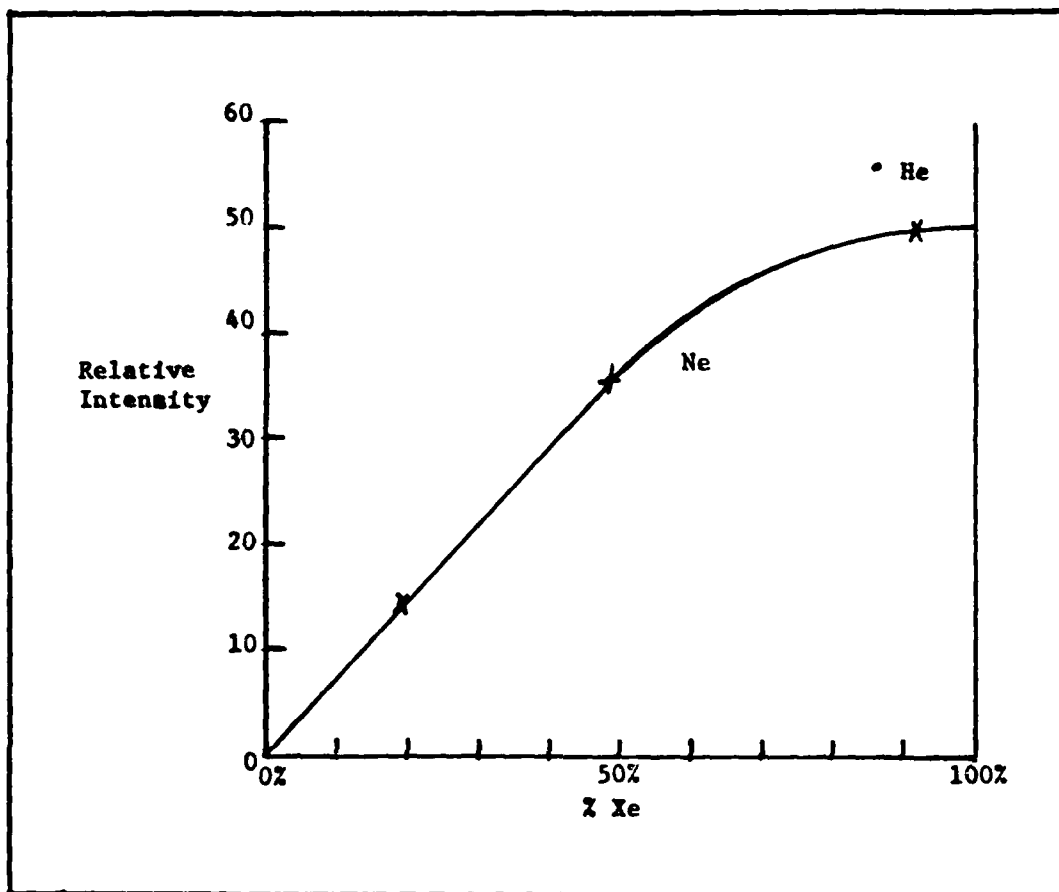


Figure 15. relative  $\text{XeCl}^*$  output vs percent xenon in hollow cathode with 4 torr total pressure, 4%  $\text{HCl}$ , 20 ma per channel, and Ne or He buffer gas.



## V. Summary and Conclusions

A hollow cathode discharge containing mixtures of neon, xenon, and hydrogen chloride has been used to produce  $\text{XeCl}^*$  excimer emissions. The hollow cathode discharge can be thought of as being beam maintained. Electrons, leaving the cathode surface, are accelerated in the sheath region, obtaining energies up to the cathode-fall voltage  $V_c$ . These beam electrons are trapped in the negative-glow region of the plasma, due to the potential well of depth  $V_c$ , and lose their energy in ionizing and exciting collisions with the buffer-gas and xenon. In the hollow cathode for this experiment, the discharge width (tube diameter) is small enough so that the electron beam created in the sheath possesses a reaching distance longer than the diameter. Hence, the beam electrons will oscillate between opposing sheaths. This beam concept provides the basis for the approximation of a spatially uniform source for electron-ion pairs throughout the negative glow. In other words, the source function  $j_e$  for creation of electron-ion pairs is due solely to beam electrons and is independent of coordinate (Ref 15: 5694).

The hollow cathode discharge contains several groups of electrons including the low density beam group with energies near the cathode-fall and a thermal group with a large number density. A third intermediate energy group can be neglected. Gerstenberger et al (Ref 13: 826) have measured the density and temperature of the low energy group and found them to be of the order of  $700^\circ \text{K}$  and  $10^{12}/\text{cm}^3$  for the discharge conditions studied here. It is because of these high electron densities that the electric field within the negative glow is very small and thus allowing a stable discharge in the presence of the electronegative  $\text{Cl}$ .

The  $\text{XeCl}^*$  excimer in the hollow cathode is formed primarily through the combination of  $\text{Xe}^+$  and  $\text{Cl}^-$ . Even though this process is relatively

slow at low pressures, it is still faster than the harpoon reaction of Xe metastables with HCl and the dissociative attachment of  $\text{Cl}^-$  with the dimer ion  $\text{Xe}_2^+$ . The harpoon reaction, in fact, reaches a limit with increasing amounts of HCl, since the HCl becomes the primary quencher of the Xe metastables. Both analytic and experimental results verify these conclusions by showing that the  $\text{XeCl}^*$  spontaneous emission intensity is a linear function of Xe concentration, HCl concentration, discharge current, and pressure.

While the hollow cathode provides an easy means for studying the  $\text{XeCl}^*$  excimer and its emissions, it is not very efficient in producing the excimer. When the  $\text{Xe}^+$  and  $\text{Cl}^-$  are attracted together at low pressures, there are two potential outcomes, excimer formation or mutual neutralization. At these pressures the excimer formation has a rate constant of  $5 \times 10^{-9} \text{ cm}^3/\text{sec}$  compared to mutual neutralization's  $2 \times 10^{-7} \text{ cm}^3/\text{sec}$ . The neutralization process is thus 250 times more probable than excimer formation.

## VI. Recommendations (Ref: 16)

Additional research is recommended for investigating the loss mechanism of HCl in XeCl discharges. One approach is to understand the dynamics of HCl and its products under discharge conditions. Changes in the dynamics can be controlled/studied with the addition of materials which act to modify the HCl loss rate. Experiments conducted by McKee (Ref: 17), for example, demonstrated that the lifetime of an  $\text{XeCl}^*$  laser containing Xe/Xe/HCl could be increased by the addition of small amounts of  $\text{H}_2$ . Winegarden (Ref: 18) also demonstrated this process but at the expense of  $\text{XeCl}^*$  total output.

The details of the rather broad-band vibrational-rotational spontaneous and laser emissions need to be treated in greater detail. This requires use of the individual branching ratios providing population of the upper laser levels. In this thesis the gross simplification has been made that the radiation processes have been treated as from a single level. The neglect of the various collisional relaxation processes is justified to some extent in that all of the hollow cathode observations were made at low pressures ( $<4$  torr). The collisional effects are much more important in the atmospheric pressure transverse excited discharges. Other effects that must be included are the collisions of the slow group of electrons (assumed to be the greatest number). Influences that must be included in a more complete model are the collisional mixing of the  $\text{XeCl(B)}$  state to the  $\text{XeCl(C)}$  state and also the direct quenching of the  $\text{XeCl(B)}$  state to the  $\text{XeCl(X)}$  state by superelastic collisions.

The importance of vibrationally excited HCl and excited states of Xe may have been underestimated in this thesis. Recent results, for example,

have shown a dramatic dependence of dissociative attachment on the vibrational level of the HCl (Ref: 19). Data from Kolts (Ref: 5) has shown that the quenching of Xe ( $6s^3P_{1,2}$ ) by HCl ( $v=0$ ) to form the XeCl (B) state is negligible. The reaction of high electronic states of Xe with HCl however, has been observed to give XeCl(B) fluorescence with a rate constant of  $1.6 \times 10^{-9} \text{ cm}^3/\text{sec}$  (Ref: 20). Likewise the reaction of Xe( $6s^3P_2$ ) with HCl ( $v = 1$ ) to form XeCl(B) has been measured recently to proceed with a rate constant of  $2 \times 10^{-10} \text{ cm}^3/\text{sec}$  (Ref 21).

There are a number of refinements which can be made in the procedures for modeling and measuring XeCl\* in the hollow cathode discharge. This thesis has not treated completely the slowing down processes of the fast cathode electrons. An improvement could be made by employing the continuous slowing down approximation (CSDA) or by a Monte Carlo calculation. Next the influence of Xe\* metastables in the contribution to the positive ionization could be included. While this is believed to be less important in the hollow cathode discharge configuration at low pressures, it becomes more important at higher pressures and energy densities. Finally the discharge could be operated in a pulsed mode. Pulsing would allow the measurement of XeCl\* output under high current densities without putting a strain on power supply and cooling requirements.

### Bibliography

1. von Engel, A. Ionized Gases, 2nd ed., Great Britain: Oxford University Press, 1965.
2. Sturges, D.J. and Oskam, H.J. "A Qualitative Theory of the Medium Pressure Hollow Cathode Effect," Physica, 37: 457-466 (1967).
3. Borodin, V.S., Kagan, Yu. M., and Lyagushchenko, R.I. "Investigation of a Hollow-Cathode Discharge. II.," Soviet Physics-Technical Physics, Vol. 11, No. 7: 887-889 (1967).
4. Hutchinson, M.H.R. "Excimers and Excimer Lasers," Applied Physics, 21: 95-114 (1980).
5. Kolts, J.H., Velasco, J.E., and Setser, D.W. "Reactive Quenching Studies of Xe ( $6s, ^3P_2$ ) Metastable Atoms by Chlorine Containing Molecules," J. Chem. Phys., 71(3): 1247-1263 (1979).
6. Ewing, J.J. "Rare-gas Halide Lasers," Physics Today: 32-39 (1978).
7. Flannery, M.R. "Atomic and Molecular Collision Processes in Rare-Gas-Halide Lasers and Rare-Gas Excimer," International Journal of Quantum Chemistry: Quantum Chemistry Symposium 13: 501-529 (1979).
8. Systems Research Laboratory. Monthly R&D Status Report. AFWAL/POOC-3, Contract F33615-79-C-2084. Dec 80 - Jan 81.
9. Finn, T.G., Chang, R.S.F., Palumbo, L.J., and Champagne, L.F. "Kinetics of the XeCl (B $\rightarrow$ X) Laser," Appl. Phys. Lett., Vol. 36, No. 10: 789-791 (1980).
10. Johnson, T.H. and Hunter, A.M., II. "Physics of the Krypton Fluoride Laser," J. Appl. Phys., 51(5): 2406-2420 (1980).
11. Rhodes, Ch. K., Editor. Excimer Lasers. Berlin: Springer-Verlag 1979.
12. Hinno, E. and Hirschberg, J.G. "Electron-Ion Recombination in Dense Plasmas," Physical Review, Vol. 125, No. 3: 795-801 (1962).
13. Gerstenberger, D.C., Solanki, R., and Collins, G.J. "Hollow Cathode Metal Ion Lasers," IEEE Journal of Quantum Electronics, Vol. QE-16, No. 8: 820-834 (1980).
14. Persson, K. "Brush Cathode Plasma--A Well-Behaved Plasma," Journal of Applied Physics, Vol. 36, No. 10: 3086-3094 (1965).

15. Warner, B.E., Persson, K., and Collins G.J. "Metal-vapor Production by Sputtering in a Hollow-cathode Discharge: Theory and Experiment," J. Appl. Phys., 50(9): 5694-5703 (1979).
16. Garscadden, A. AF Wright Aeronautical Laboratories, Energy Conversion Branch (private communication).
17. McKee, T.J., James, D.J., Nip, W.S., Weeks, R.W., and Willis, C. Applied Phys Lett., 36: 943 (1980).
18. Winegarden, J. Master of Science Thesis. Air Force Institute of Technology (1980). Measurement of  $Cl_2$  Concentration in a XeCl Hollow Cathode Discharge including the Effect of  $H_2$  Addition.
19. Allen, M., Wong, S.F. J. Chem. Phys. 74, 1687 (1981)
20. Setser, D.W. Proc. 334d Gaseous Electronics Conference, Norman, Oklahoma 1980.
21. Chang, R.S. Naval Research Laboratory, Washington D.C. (to be published)

### Vita

George A. Vogel, Jr. was born on 9 March 1949 in Toledo, Ohio. He is the son of Mr. and Mrs. George A. Vogel of Suttons Bay, Michigan. In June 1967 he graduated from Xenia High School, Xenia, Ohio. He received a B.S. degree in Electrical Engineering from the University of Cincinnati, Cincinnati, Ohio in 1972. He began working for the Air Force Avionics Laboratory, Electromagnetic Warfare Division in June 1972. He entered the Air Force Institute of Technology in June 1976 as a part time student. He was married to his wife, Donna, on 10 June 1977.

Permanent Address: P.O. 128  
Beavercreek, OH  
45301

This thesis was typed by Mrs. Judy Tislow.

UNCLASSIFIED

SECURITY CLASSIFICATION OF THIS PAGE (When Data Entered)

| REPORT DOCUMENTATION PAGE   |                                     | READ INSTRUCTIONS<br>BEFORE COMPLETING FORM                    |
|---|-------------------------------------|--|
| 1. REPORT NUMBER<br>AFIT/GEP/81-6   | 2. GOVT ACCESSION NO.<br>AD-A103348 | 3. RECIPIENT'S CATALOG NUMBER                                  |
| 4. TITLE (and Subtitle)<br>Analysis of XeCl Emission in a<br>Hollow Cathode Discharge   |                                     | 5. TYPE OF REPORT & PERIOD COVERED<br>MS Thesis                |
|   |                                     | 6. PERFORMING ORG. REPORT NUMBER                               |
| 7. AUTHOR(s)<br>George A. Vogel, Jr.  |                                     | 8. CONTRACT OR GRANT NUMBER(s)                                 |
| 9. PERFORMING ORGANIZATION NAME AND ADDRESS<br>Air Force Institute of Technology (AFIT-EN)<br>Wright-Patterson AFB, OH 45433  |                                     | 10. PROGRAM ELEMENT, PROJECT, TASK<br>AREA & WORK UNIT NUMBERS |
| 11. CONTROLLING OFFICE NAME AND ADDRESS   |                                     | 12. REPORT DATE<br>June 1981                                   |
|   |                                     | 13. NUMBER OF PAGES  |
| 14. MONITORING AGENCY NAME & ADDRESS (if different from Controlling Office)   |                                     | 15. SECURITY CLASS. (of this report)<br><br>UNCLASSIFIED       |
|   |                                     | 15a. DECLASSIFICATION/DOWNGRADING<br>SCHEDULE                  |
| 16. DISTRIBUTION STATEMENT (of this Report)<br><br>Approved for public release; distribution unlimited.   |                                     |  |
| 17. DISTRIBUTION STATEMENT (of the abstract entered in Block 20, if different from Report)  |                                     |  |
| 18. SUPPLEMENTARY NOTES<br>Approved for public release, IAW AFR 190-17<br>FREDRICK C. LYNCH, Major, USAF<br>Director of Public Affairs<br>13 AUG 1981 <i>Fredrick C. Lynch</i><br>Air Force Institute of Technology (ATC)<br>Wright-Patterson AFB, OH 45433   |                                     |  |
| 19. KEY WORDS (Continue on reverse side if necessary and identify by block number) <b>FREDRICK C. LYNCH, Major, USAF</b><br>Director of Public Affairs<br>Hollow Cathode Discharge<br>XeCl<br>Excimer   |                                     |  |
| 20. ABSTRACT (Continue on reverse side if necessary and identify by block number)<br>This work investigates the characteristics of a hollow cathode discharge containing neon, xenon, and hydrogen chloride gases. The line intensity of the XeCl excimer spontaneous emission (308 nm) is measured as a function of excitation current and the partial pressures of Xe and HCl.<br>The hollow cathode, operating with constant discharge current, produces relatively intense XeCl emission and provides a stable discharge, in spite of the presence of the electronegative Cl ions. Measurements were made for<br>(Cont..) |                                     |  |

DD FORM 1473

1 JAN 73

EDITION OF 1 NOV 65 IS OBSOLETE

UNCLASSIFIED

SECURITY CLASSIFICATION OF THIS PAGE (When Data Entered)



UNCLASSIFIED

SECURITY CLASSIFICATION OF THIS PAGE(When Data Entered)

total pressures of 4, 2, and 1 torr, 0, 2, 4, and 8 percent HCl, and mixes of Ne/Xe from 100% Ne to 100% Xe.

The hollow cathode provides a unique discharge characteristic by providing both 200 - 400 ev "beam like" electrons and high densities ( $10^{12}/\text{cm}^3$ ) of low energy (700°K) electrons. A simple model is developed for the hollow cathode discharge by assuming the electrons are only in these two energy groups. This model is coupled with the dominant chemical processes and is used to explain the behavior of the discharge with direct current excitation.

The results of both analysis and measurements show the XeCl emission to be proportional to Xe concentration, HCl concentration, and discharge current. These results indicate that the primary formation process of the XeCl excimer in the hollow cathode is due to the combination of Xe and Cl ions.

SECURITY CLASSIFICATION OF THIS PAGE(When Data Entered)

DATE  
FILMED  
-8